On the significance of sulphuric-acid dissociation in the modelling of vanadium redox flow batteries

MICHAEL VYNNYCKY, Milton Assunção

Journal of Engineering Mathematics manuscript No.
(will be inserted by the editor)

On the significance of sulphuric-acid dissociation in the modelling of vanadium redox flow batteries

M. Vynnycky · **M. Assunção**

Received: date / Accepted: date

Abstract A recent asymptotic model for the operation of a vanadium redox flow battery (VRFB) is extended to include the dissociation of sulphuric acid - a bulk chemical reaction that occurs in the battery's porous flow-through electrodes, but which is often omitted from VRFB models. Using asymptotic methods and time-dependent two-dimensional numerical simulations, we show that the charge-discharge curve for the model with the dissociation reaction is almost identical to that for the model without, even though the concentrations of the ionic species in the recirculating tanks, although not the state of charge, are considerably different in the two models. The ability of the asymptotic model to extract both the qualitative and quantitative behaviour of the considerably more time-consuming numerical simulations correctly indicates that it should be possible to add further physical phenomena to the model without incurring significant computational expense.

Keywords Vanadium redox flow battery · Electrochemistry · Asymptotic analysis

1 Introduction

Current demand for increasingly efficient renewable energy delivery has generated substantial interest in vanadium redox flow batteries (VRFBs) as an energy storage technology. VRFBs have numerous potential applications: load levelling and peak shaving, uninterruptible power supplies, emergency backup and facilitation of wind and photovoltaic energy delivery.

M. Vynnycky (Corresponding author)
Department of Mathematics and Statistics, University of Limerick, Limerick, V94 T9PX, Ireland,
E-mail: michael.vynnycky@ul.ie

M. Assunção
Department of Applied Mathematics and Statistics, Institute of Mathematical and Computer Sciences, University of São Paulo at São Carlos, 13560-970 São Carlos, São Paulo, Brazil,
E-mail: assuncao@icmc.usp.br

A VRFB consists of an assembly of cells, typically referred to as a stack; one such cell is shown in Fig. 1. It is composed of positive and negative flow-through electrodes, typically made of porous carbon felt, that are separated by a proton exchange membrane that consists of charged molecules: the mobile protons that pass through it and fixed sites of negative charge. During operation, vanadium-based electrolytes are pumped through the electrodes; the electrolyte in the positive electrode, vanadyl sulphate ($VOSO_4$), contains VO_2^+ and VO^{2+} ions, whilst that in the negative electrode, vanadium sulphate ($V_2(SO_4)_3$), contains V^{2+} and V^{3+} ions. In addition, both electrodes are connected to pumps and storage tanks, meaning that very large electrolyte volumes can be circulated through the cell. During charging, the VO^{2+} ions in the positive electrode are reduced to VO_2^+ ions, and electrons exit from the positive terminal of the cell via a current collector that bounds the electrode on the side opposite to that of the membrane. Similarly, in the negative electrode, electrons enter via another current collector, reducing the V^{3+} ions to V^{2+} ions; during discharge, the reverse process, also known as oxidation, occurs. Charging and discharging can be written as

$$V^{3+} + e^- \underset{\text{discharge}}{\overset{\text{charge}}{\rightleftharpoons}} V^{2+} \quad \text{at the negative electrode,} \tag{1.1}$$

$$VO^{2+} + H_2O \underset{\text{discharge}}{\overset{\text{charge}}{\rightleftharpoons}} VO_2^+ + e^- + 2H^+ \quad \text{at the positive electrode.} \tag{1.2}$$

Typically, each cell in a VRFB operates at a nominal voltage in the interval 1.15-1.55 V and at a temperature of around 30^{o}C.

Mathematical modelling and numerical simulation have recently come to play an increasingly important role in VRFB research and development. In general, the models in question consist of a system of partial differential equations that describe the transient mass, momentum and charge transport that occur in the processes mentioned above [1–15], and invariably require numerical solution. However, recent work by Vynnycky and Assunção [16] demonstrated that a standard and often-used VRFB model could be reduced asymptotically to give a much simpler set of equations which had a quasi-analytical solution; moreover, the reduced model was found to require around 250 times less computational time than the original one. Having said that, the model considered only the global mechanism described by reactions (1.1) and (1.2), which makes sense in light of the uncertainty in the kinetics and a lack of characterization of material parameters. Nevertheless, other phenomena are also believed to be at play: oxygen and hydrogen evolution via the gas-evolving side-reactions [4, 5, 17]

$$2H_2O + 2e^- \rightleftharpoons H_2 + 2OH \quad (\text{hydrogen evolution}),$$

$$2H_2O \rightleftharpoons O_2 + 4e^- + 4H^+ \quad (\text{oxygen evolution});$$

thermal effects [2,10–13]; acid dissociation [9,18,19]; vanadium crossover [9], whereby V^{2+} and V^{3+} ions are transported from the negative electrode across the membrane

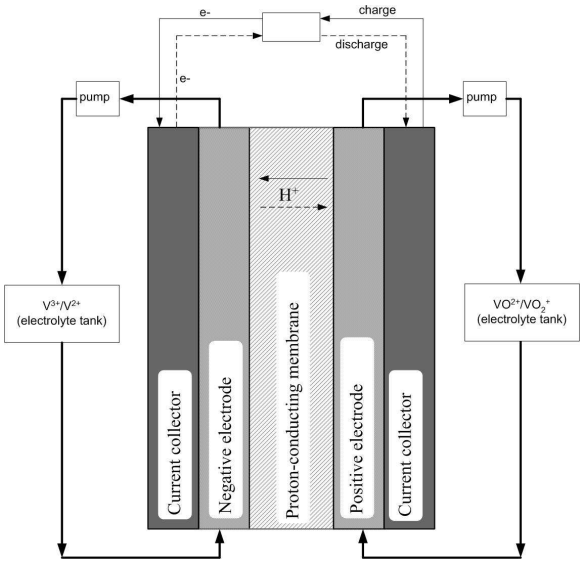

Fig. 1 A schematic of the overall operation of a vanadium redox flow battery

to the positive electrode, and VO_2^+ and VO^{2+} ions are transported the other way; and a further positive-electrode side-reaction [1, 17]

$$VO^{2+} + 2H_2O \rightleftharpoons HVO_3 + 3H^+ + e^-.$$

Thus, it would be of interest to see if any or all of these, amongst others, can be incorporated into the asymptotic framework of [16], especially in view of the computational advantage of doing so. In this light, we focus in this paper on the dissociation of sulphuric acid (H_2SO_4), as this is the mechanism that is included in the VRFB starting model available in the commercially available finite element software Comsol Multiphysics [20]. This is normally treated as a two-step reaction in which the first dissociation step,

$$H_2SO_4 \rightarrow H^+ + HSO_4^-, \tag{1.3}$$

is assumed to be complete, whereas the second, given by

$$HSO_4^- \rightarrow H^+ + SO_4^{2-}, \tag{1.4}$$

is not.

The layout of the paper is as follows. In Sect. 2, we formulate a transient two-dimensional (2D) model for VRFB operation, extending the description in [16] to include the dissociation of sulphuric acid; in Sect. 3, the governing equations are nondimensionalized. In Sect. 4, we carry out an asymptotic analysis of the problem, and present the results in Sect. 5, with conclusions being drawn in Sect. 6.

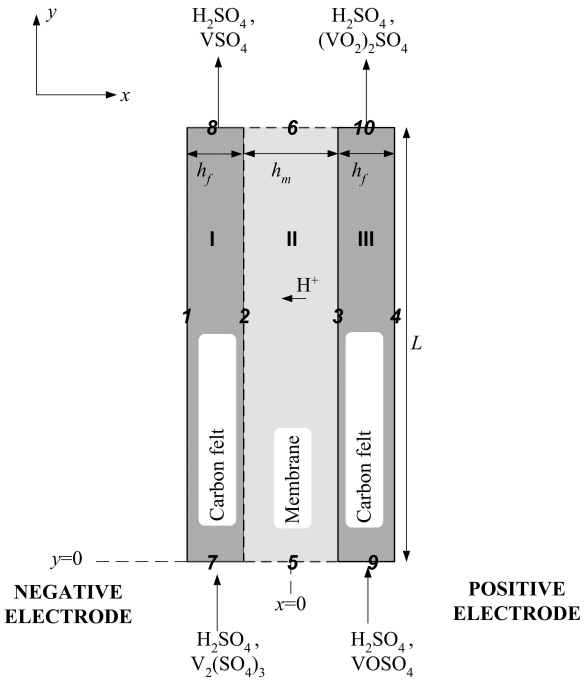

Fig. 2 A schematic of a VRFB during charging. **I-III** represent the components of the cell, whereas ***1-10*** represent internal interfaces or external boundaries.

2 Mathematical model

As in [16], we consider a model geometry consisting of positive and negative porous flow-through electrodes and a proton exchange membrane, as shown in Fig. 2. As well as the presence of V^{2+} and V^{3+} ions at the negative electrode and VO^{2+} and VO_2^+ ions at the positive electrode, owing to reactions (1.1) and (1.2), it is natural to assume the presence of H^+, HSO_4^- and SO_4^{2-} ions in both electrodes, as a result of the partial dissociation of dilute sulphuric acid. In addition, we assume that: the geometry is two-dimensional; the cell is isothermal; the membrane is fully humidified; H^+ ions can cross over the membrane, but all other ions cannot; the dilute-solution approximation is valid; the porosities of each electrode are constant and identical. The rationale behind these assumptions is given at length in [16], and therefore not repeated here.

2.1 Governing equations

*2.1.1 Porous carbon electrodes (**I**,**III**)*

The molar flux, $\mathbf{N}_k$, of ionic species k in a porous medium of porosity, ε, can be expressed via a modified Nernst-Planck equation as

$$\mathbf{N}_k = c_k u^{\text{in}} \mathbf{e}_y - \frac{z_k c_k D_k^{\text{eff}} F}{RT} \nabla \phi_{\text{e}} - D_k^{\text{eff}} \nabla c_k, \tag{2.1}$$

where c_k denotes the concentration of species k, u^{in} is the velocity of the electrolyte at the inlet, $\mathbf{e}_y$ is the unit vector in the y-direction, ϕ_{e} is the electric potential in the electrolyte, z_k is the charge number for species k, and D_k^{eff} is the effective diffusion coefficient for species k, which is related to the usual diffusion coefficient, D_k, by the Bruggeman relation,

$$D_k^{\text{eff}} = \varepsilon^{3/2} D_k; \tag{2.2}$$

in addition, the quantities F, R and T are Faraday's constant, the universal gas constant and the absolute temperature, respectively. The three terms on the right-hand side of Eq. (2.1) represent ionic transport due to convection, migration and diffusion. The form used for the convection term already supposes identical plug flows in each porous electrode [16, 21, 22]. The volume-averaged differential material balance in the porous carbon electrodes for species k is then expressed as

$$\varepsilon \frac{\partial c_k}{\partial t} + \nabla \cdot \mathbf{N}_k = -(S_k + R_k), \tag{2.3}$$

where t is time, S_k is the electrochemical reaction source term for species k and R_k is the source term associated with homogeneous chemical reactions; the explicit forms for these will be given shortly. Also, assuming that the electrolyte is electroneutral gives

$$\sum_k z_k c_k = 0. \tag{2.4}$$

Also, since the charge entering the electrolyte must be balanced by that which leaves the solid phase of the electrode, we have

$$\nabla \cdot \mathbf{i}_{\text{e}} + \nabla \cdot \mathbf{i}_{\text{s}} = 0, \tag{2.5}$$

where $\mathbf{i}_e$ and $\mathbf{i}_{\text{s}}$ are the ionic and electronic current densities, respectively. Moreover, $\mathbf{i}_{\text{e}}$ is given by

$$\mathbf{i}_{\text{e}} = \sum_k z_k F \mathbf{N}_k, \tag{2.6}$$

whereas $\mathbf{i}_{\text{s}}$ is given by Ohm's law, i.e.

$$\mathbf{i}_{\text{s}} = -\sigma_{\text{s}}^{\text{eff}} \nabla \phi_{\text{s}}, \tag{2.7}$$

where ϕ_{s} is the electronic potential and $\sigma_{\text{s}}^{\text{eff}}$ is the effective electronic conductivity of the porous electrode, which is related to the electronic conductivity of solid material, σ_{s}, by a further Bruggeman relation,

$$\sigma_{\text{s}}^{\text{eff}} = (1-\varepsilon)^{3/2} \sigma_{\text{s}}. \tag{2.8}$$

More particularly, (2.5) is rewritten as

$$\nabla \cdot \mathbf{i}_{\mathrm{e}} = j_-, \quad \nabla \cdot \mathbf{i}_{\mathrm{s}} = -j_- \tag{2.9}$$

for the negative electrode, region **I** in Fig. 2, and

$$\nabla \cdot \mathbf{i}_{\mathrm{e}} = j_+, \quad \nabla \cdot \mathbf{i}_{\mathrm{s}} = -j_+ \tag{2.10}$$

for the positive electrode (region **III**), where j_- and j_+ are transfer current densities for the electrochemical reactions that occur at the surfaces of the porous electrodes. As in [1, 9], j_- and j_+ are expressed via the Butler-Volmer relations,

$$j_- = AFk_- \left(c^s_{\mathrm{V}^{2+}}\right)^{\alpha_{-,\mathrm{c}}} \left(c^s_{\mathrm{V}^{3+}}\right)^{\alpha_{-,\mathrm{a}}} \left\{ \exp\left(\frac{\alpha_{-,\mathrm{a}} F\eta_-}{RT}\right) - \exp\left(-\frac{\alpha_{-,\mathrm{c}} F\eta_-}{RT}\right) \right\}, \tag{2.11}$$

$$j_+ = AFk_+ \left(c^s_{\mathrm{VO}^{2+}}\right)^{\alpha_{+,\mathrm{c}}} \left(c^s_{\mathrm{VO}^+_2}\right)^{\alpha_{+,\mathrm{a}}} \left\{ \exp\left(\frac{\alpha_{+,\mathrm{a}} F\eta_+}{RT}\right) - \exp\left(-\frac{\alpha_{+,\mathrm{c}} F\eta_+}{RT}\right) \right\}, \tag{2.12}$$

where A is the specific electroactive area, k_- and k_+ are reaction rate constants, $\alpha_{\pm,a}$ and $\alpha_{\pm,c}$ are the anodic and cathodic apparent transfer coefficients for reactions (1.1) and (1.2), respectively, and η_+ and η_- are the overpotentials, given by

$$\eta_\pm = \phi_{\mathrm{s}} - \phi_{\mathrm{e}} - E_\pm, \tag{2.13}$$

with E_- and E_+ as, respectively, the equilibrium potentials for reactions (1.1) and (1.2), which are in turn given by

$$E_- = E_{0,-} - \frac{RT}{F} \ln\left(\left(c_{\mathrm{V}^{2+}}\right)^{s_{\mathrm{V}^{2+}}} \left(c_{\mathrm{V}^{3+}}\right)^{s_{\mathrm{V}^{3+}}} \right), \tag{2.14}$$

$$E_+ = E_{0,+} - \frac{RT}{F} \ln\left(\left(c_{\mathrm{VO}^{2+}}\right)^{s_{\mathrm{VO}^{2+}}} \left(c_{\mathrm{VO}^+_2}\right)^{s_{\mathrm{VO}^+_2}} \left(c_{\mathrm{H}^+}\right)^{s_{\mathrm{H}^+}} \right), \tag{2.15}$$

respectively; in addition, $E_{0,-}$ and $E_{0,+}$ denote the equilibrium potentials at standard conditions for reactions (1.1) and (1.2), respectively. In Eqs. (2.11) and (2.12), the quantities $c^s_{\mathrm{V}^{3+}}, c^s_{\mathrm{V}^{2+}}, c^s_{\mathrm{VO}^{2+}}$ and $c^s_{\mathrm{VO}^+_2}$ represent the concentrations of these species at the electrode/electrolyte interface; this value usually differs from that within the bulk of the electrolyte due to the additional resistance to the transport of species from the interior bulk to the interfaces [1, 11], and is given by

$$c^s_i = \frac{c_i + \varepsilon k_- e^{-\alpha_{-,\mathrm{c}} F\eta_-/RT} (c_{\mathrm{V}^{2+}}/\gamma_{\mathrm{V}^{3+}} + c_{\mathrm{V}^{3+}}/\gamma_{\mathrm{V}^{2+}})}{1 + \varepsilon k_- (e^{-\alpha_{-,\mathrm{c}} F\eta_-/RT}/\gamma_{\mathrm{V}^{2+}} + e^{\alpha_{-,\mathrm{a}} F\eta_-/RT}/\gamma_{\mathrm{V}^{3+}})}, \quad i = \mathrm{V}^{2+}, \mathrm{V}^{3+}, \tag{2.16}$$

$$c^s_i = \frac{c_i + \varepsilon k_+ e^{-\alpha_{+,\mathrm{c}} F\eta_+/RT} (c_{\mathrm{VO}^{2+}}/\gamma_{\mathrm{VO}^+_2} + c_{\mathrm{VO}^+_2}/\gamma_{\mathrm{VO}^{2+}})}{1 + \varepsilon k_+ (e^{-\alpha_{+,\mathrm{c}} F\eta_+/RT}/\gamma_{\mathrm{VO}^+_2} + e^{\alpha_{+,\mathrm{a}} F\eta_+/RT}/\gamma_{\mathrm{VO}^{2+}})}, \quad i = \mathrm{VO}^+_2, \mathrm{VO}^{2+}, \tag{2.17}$$

where $\gamma_k = D_k/d_f$, with d_f as the average distance between the fibres of the carbon felt. Furthermore, Eqs. (2.11) and (2.12), together with the stoichiometric coefficients

Source term	Positive electrode	Negative electrode
S_{H^+}	$s_{H^+} j_+/F$	0
$S_{HSO_4^-}$	0	0
$S_{SO_4^{2-}}$	0	0
$S_{V^{2+}}$	-	$s_{V^{2+}} j_-/F$
$S_{V^{3+}}$	-	$s_{V^{3+}} j_-/F$
$S_{VO^{2+}}$	$s_{VO^{2+}} j_+/F$	-
$S_{VO_2^+}$	$s_{VO_2^+} j_+/F$	-

Table 1 Source and sink terms for electrochemical reactions in equation (2.3)

Source term	Positive electrode	Negative electrode
R_{H^+}	$-r_d$	$-r_d$
$R_{HSO_4^-}$	r_d	r_d
$R_{SO_4^{2-}}$	$-r_d$	$-r_d$
$R_{V^{2+}}$	-	0
$R_{V^{3+}}$	-	0
$R_{VO^{2+}}$	0	-
$R_{VO_2^+}$	0	-

Table 2 Source and sink terms for homogeneous chemical reactions in equation (2.3)

Parameter	Value	Units	Reference
c_{fcs}	1990	mol m^{-3}	[23]
$E_{0,+}$	1.004	V	[24]
$E_{0,-}$	-0.255	V	[24]
k_+	2.5×10^{-8}	m s^{-1}	[17]
k_-	7×10^{-8}	m s^{-1}	[1]
k_d	1×10^{4}	mol m^{-3}s^{-1}	[9]
s_{H^+}	-2	-	-
$s_{V^{2+}}$	1	-	-
$s_{V^{3+}}$	-1	-	-
$s_{VO^{2+}}$	1	-	-
$s_{VO_2^+}$	-1	-	-
z_{fcs}	-1	-	-
z_{H^+}	1	-	-
$z_{HSO_4^-}$	-1	-	-
$z_{SO_4^{2-}}$	-2	-	-
$z_{V^{2+}}$	2	-	-
$z_{V^{3+}}$	3	-	-
$z_{VO^{2+}}$	2	-	-
$z_{VO_2^+}$	1	-	-
$\alpha_{\pm,c}$	0.45	-	[9]
$\alpha_{\pm,a}$	0.55	-	[9]
β	0.25	-	[25]

Table 3 Default values of chemical and electrochemical constants

Parameter	Value	Units
$c^{0,-}_{H^+}, c^{0,+}_{H^+}$	4447.5*, 5097.5†	mol m^{-3}
$c^0_{HSO_4^-}$	2668.5*, 3058.5†	mol m^{-3}
$c^0_{SO_4^{2-}}$	2371.5*, 1981.5†	mol m^{-3}
$c^0_{V^{2+}}$	156	mol m^{-3}
$c^0_{V^{3+}}$	884	mol m^{-3}
$c^0_{VO^{2+}}$	884	mol m^{-3}
$c^0_{VO_2^+}$	156	mol m^{-3}

Table 4 Default initial values (*negative electrode; †positive electrode). All parameter values are taken from [9].

Parameter	Value	Units
A	3.5×10^{4}	m^{-1}
d_{f}	1×10^{-5}	m
h_{f}	4×10^{-3}	m
h_{m}	2.03×10^{-4}	m
L	0.035	m
u^{in}	4.7×10^{-3}	m s^{-1}
V	5.6×10^{-5}	m^3
W	2.85×10^{-2}	m
ε	0.93	-

Table 5 Default geometry-related parameters, as in [9].

Parameter	Value	Units	Reference
D_{H^+}	9.31×10^{-9}	m^{2}s^{-1}	[26]
$D_{H^+,\mathrm{m}}$	3.35×10^{-9}	m^{2}s^{-1}	[9]
$D_{HSO_4^-}$	1.39×10^{-9}	m^{2}s^{-1}	[27]
$D_{SO_4^{2-}}$	1.07×10^{-9}	m^{2}s^{-1}	[27]
$D_{V^{2+}}$	2.4×10^{-10}	m^{2}s^{-1}	[28]
$D_{V^{3+}}$	2.4×10^{-10}	m^{2}s^{-1}	[28]
$D_{VO^{2+}}$	3.9×10^{-10}	m^{2}s^{-1}	[28]
$D_{VO_2^+}$	3.9×10^{-10}	m^{2}s^{-1}	[28]
F	96485	Cmol^{-1}	-
i_{app}	400	A m^{-2}	[9]
R	8.314	Jmol^{-1}K^{-1}	-
T	300	K	[9]
σ_{m}	24.9	S m^{-1}	*
$\sigma_{\mathrm{s}}^{\mathrm{eff}}$	66.7	S m^{-1}	[9]

Table 6 Default values for constants related to transport of charge and mass (* based on the values of $D_{H^+,\mathrm{m}}$ and c_{H^+} in [9] and [23], respectively)

in (1.1) and (1.2), are used to constitute the terms for S_k in Eq. (2.3), which are given in Tables 1 and 3.

As for the dissociation of sulphuric acid, this is described by means of a source term, r_d, given by

$$r_d = k_d \left(\frac{c_{\mathrm{H}^+} - c_{\mathrm{HSO}_4^-}}{c_{\mathrm{H}^+} + c_{\mathrm{HSO}_4^-}} - \beta \right), \tag{2.18}$$

where k_d is a rate parameter and β the degree of dissociation; typically used values for these are given in Table 3, and Table 2 shows how r_d enters the governing equations. Note, however, that [9, 18, 19] document this reaction incorrectly in different ways; in [9], the conservation equation the sulphate ion in their model is not explicitly given, as this ion is removed via the electroneutrality equations, whereas [18,19] include the sulphate ion, but do not indicate that they include homogeneous reaction term for this ion in the conservation equation.

*2.1.2 Membrane (**III**)*

First of all, unlike the electrolyte in the porous electrodes, the liquid in the membrane, which is assumed to consist of water and protons, is not electroneutral. However, electroneutrality can be assumed to hold when the fixed negative charge sites in the membrane structure are taken into account; hence,

$$z_{\mathrm{H}^+} c_{\mathrm{H}^+} + z_{\mathrm{fcs}} c_{\mathrm{fcs}} = 0, \tag{2.19}$$

where z_{fcs} is the charge of the fixed sites and c_{fcs} is their concentration, which is here assumed to be constant.

Current conservation gives

$$\nabla \cdot \mathbf{i}_{\mathrm{m}} = 0, \tag{2.20}$$

where $\mathbf{i}_{\mathrm{m}}$ is the ionic current density, and is given by

$$\mathbf{i}_{\mathrm{m}} = z_{\mathrm{H}^+} F \mathbf{N}_{\mathrm{H}^+}, \tag{2.21}$$

with

$$\mathbf{N}_{\mathrm{H}^+} = -\frac{z_{\mathrm{H}^+} F c_{\mathrm{H}^+} D_{\mathrm{H}^+,\mathrm{m}}}{RT} \nabla \phi_{\mathrm{m}}, \tag{2.22}$$

where $D_{\mathrm{H}^+,\mathrm{m}}$ is the proton diffusion coefficient in the membrane; however, since Eq. (2.19) implies that c_{H^+} is constant in the membrane, this results in

$$\nabla^2 \phi_{\mathrm{m}} = 0. \tag{2.23}$$

Note that combining (2.21) and (2.22) gives, in effect, Ohm's law for the membrane, and we can therefore identify the electrical conductivity of the membrane, σ_{m}, as being given by

$$\sigma_{\mathrm{m}} = F^2 c_{\mathrm{H}^+} D_{\mathrm{H}^+,\mathrm{m}} / RT. \tag{2.24}$$

Moreover, the above description, which considers proton migration as the only transport process in the membrane, is perhaps one of the simplest available [23], but it suffices for present purposes.

2.2 Boundary and interfacial conditions

*2.2.1 Current collector/porous felt interface in the negative electrode (**1**)*

At this boundary, which corresponds to $x = -(h_\mathrm{f} + h_\mathrm{m}/2)$, the electronic potential is assigned a zero reference value and all of the ionic species have zero normal flux; thus,

$$\phi_\mathrm{s} = 0, \tag{2.25}$$

$$\mathbf{N}_k \cdot \mathbf{n} = 0, \quad k = \mathrm{H}^+, \mathrm{HSO}_4^-, \mathrm{SO}_4^{2-}, \mathrm{V}^{2+}, \mathrm{V}^{3+}. \tag{2.26}$$

In Eq. (2.26) and below, **n** denotes the unit outward normal vector at the boundary under discussion.

*2.2.2 Porous felt/membrane interface in the negative electrode (**2**)*

Here, corresponding to $x = -h_\mathrm{m}/2$, there is zero electronic current density and zero normal flux for all of the ionic species, other than H^+; these are expressed by

$$\mathbf{i}_\mathrm{s} \cdot \mathbf{n} = 0, \tag{2.27}$$

$$\mathbf{N}_k \cdot \mathbf{n} = 0, \quad k = \mathrm{HSO}_4^-, \mathrm{SO}_4^{2-}, \mathrm{V}^{2+}, \mathrm{V}^{3+}, \tag{2.28}$$

respectively. A further two conditions are required. These are continuity for the ionic current density, i.e.

$$\mathbf{i}_\mathrm{m} \cdot \mathbf{n} = \mathbf{i}_\mathrm{e} \cdot \mathbf{n}, \tag{2.29}$$

which is a consequence of Eq. (2.28) and the continuity of proton flux, and

$$\phi_\mathrm{m} = \phi_\mathrm{e} - \frac{RT}{F}\left[-\ln c_{\mathrm{H}^+}\right]_-^+, \tag{2.30}$$

where $[\quad]_-^+$ denotes the difference in the value of a function to the right (+) and the left (-) of $x = -h_\mathrm{m}/2$; Eq. (2.30) takes into account the Donnan potential which represents the potential jump at the membrane/electrolyte interface for a system in equilibrium [9].

*2.2.3 Porous felt/membrane interface in the positive electrode (**3**)*

Here, where $x = h_\mathrm{m}/2$, the interfacial conditions are similar to those at $x = -h_\mathrm{m}/2$; hence,

$$\mathbf{i}_\mathrm{s} \cdot \mathbf{n} = 0, \tag{2.31}$$

$$\mathbf{N}_k \cdot \mathbf{n} = 0, \quad k = \mathrm{HSO}_4^-, \mathrm{SO}_4^{2-}, \mathrm{VO}_2^+, \mathrm{VO}^{2+}. \tag{2.32}$$

$$[\mathbf{N}_{\mathrm{H}^+} \cdot \mathbf{n}]_-^+ = 0, \tag{2.33}$$

$$\phi_\mathrm{m} = \phi_\mathrm{e} - \frac{RT}{F}\left[\ln c_{\mathrm{H}^+}\right]_-^+, \tag{2.34}$$

with the notation $[\quad]_-^+$ now being applied at $x = h_\mathrm{m}/2$.

2.2.4 Current collector/porous felt interface in the positive electrode (**4**)

Here, at $x = h_m/2 + h_f$, the interfacial conditions are similar to (2.25) and (2.26); hence,

$$\phi_s = E_{cell}, \quad \mathbf{i}_e \cdot \mathbf{n} = 0, \tag{2.35}$$

$$\mathbf{N}_k \cdot \mathbf{n} = 0, \quad \text{for } k = H^+, HSO_4^-, SO_4^{2-}, VO_2^+, VO^{2+}, \tag{2.36}$$

where E_{cell} is the cell potential and is such that

$$\left.\begin{array}{l} E_{cell} < E_+ - E_- \text{ (discharge)} \\ E_{cell} > E_+ - E_- \text{ (charge)} \end{array}\right\}. \tag{2.37}$$

If E_{cell} is constant, then the VRFB is said to be in potentiostatic operation; however, here, as in [16], we consider galvanostatic operation, so that Eq. (2.35) is replaced by

$$\mathbf{i}_s \cdot \mathbf{n} = i_{app}, \tag{2.38}$$

where i_{app} is the applied constant current density. Moreover, in terms of i_{app}, (2.37) corresponds to

$$\left.\begin{array}{l} i_{app} < 0 \text{ (discharge)} \\ i_{app} > 0 \text{ (charge)} \end{array}\right\}. \tag{2.39}$$

Mathematically, this means that E_{cell} is a function of y and t which has to be determined as part of the solution to the overall problem; however, since the electrical conductivity of the current collectors is typically much greater than that of all other components, E_{cell} is practically a function of t alone. For generality, however, we keep i_{app} as a function of t, as allow us to derive a stronger result without any significant additional algebra, although the results in Sect. 5 will be for a constant value of i_{app}.

2.2.5 Remaining two sides of the membrane (**5**,**6**)

For these boundaries, which are located at $y = 0$ and L for $-h_m/2 \le x \le h_m/2$, there is electrical insulation, so that

$$\mathbf{i}_m \cdot \mathbf{n} = 0. \tag{2.40}$$

2.2.6 Negative electrode inlet (**7**)

At this boundary, which is located at $y = 0$ for $-(h_f + h_m/2) \le x \le -h_m/2$, we assume no outflow of either ionic or electronic current; thus,

$$\mathbf{i}_s \cdot \mathbf{n} = 0, \quad \mathbf{i}_e \cdot \mathbf{n} = 0. \tag{2.41}$$

In addition, all of the concentrations of the ionic species are prescribed, so that

$$c_k = c_k^{in}(t), \quad k = H^+, HSO_4^-, SO_4^{2-}, V^{2+}, V^{3+}, \tag{2.42}$$

where c_k^{in} is the negative electrode inlet ionic concentration for species k. The functions $c_k^{in}(t)$, which must be solved for as part of the solution to the problem, are

determined using a mass balance that assumes instantaneous mixing and negligible reaction in the tanks and relates the change of concentration in the tanks to the product of the flow rate and difference between the inlet and outlet concentrations [1]; hence,

$$V\frac{\mathrm{d}c_k^{\mathrm{in}}}{\mathrm{d}t} = \omega\left(c_k^{\mathrm{out}}(t) - c_k^{\mathrm{in}}(t)\right), \tag{2.43}$$

where V is the tank volume, ω is the volumetric flow rate and c_k^{out} is the average outlet concentration of species k, which is in turn given by

$$c_k^{\mathrm{out}}(t) = \frac{1}{h_{\mathrm{f}}}\int_{-(h_{\mathrm{m}}/2+h_{\mathrm{f}})}^{-h_{\mathrm{m}}/2} (c_k)_{y=L}\,\mathrm{d}x \quad \text{for the negative electrode;} \tag{2.44}$$

note that ω is related to u^{in} by $\omega = h_{\mathrm{f}} W \varepsilon u^{\mathrm{in}}$, where W denotes the width of the inlet in the direction perpendicular to x and y. Moreover, the inlet concentrations are used to constitute the state of charge of the system, SOC. However, as discussed in [16], there are at least three possible definitions of this, depending on whether one considers the negative electrode, the positive electrode or both electrodes; to limit the discussion, we will consider the first two, giving the expressions

$$\mathrm{SOC}_- = \frac{c^{\mathrm{in}}_{\mathrm{V}^{2+}}}{c^{\mathrm{in}}_{\mathrm{V}^{2+}} + c^{\mathrm{in}}_{\mathrm{V}^{3+}}}, \quad \mathrm{SOC}_+ = \frac{c^{\mathrm{in}}_{\mathrm{VO}_2^+}}{c^{\mathrm{in}}_{\mathrm{VO}^{2+}} + c^{\mathrm{in}}_{\mathrm{VO}_2^+}}, \tag{2.45}$$

respectively. Furthermore, $c_k^{\mathrm{out}}(t)$ is not known *a priori*, but must also be solved for as part of the problem; for this, we need boundary conditions at $y = L$, which we turn to next.

*2.2.7 Negative electrode outlet (**8**)*

At this boundary, which is located at $y = L$, $-(h_{\mathrm{f}} + h_{\mathrm{m}}/2) \le x \le -h_{\mathrm{m}}/2$, we assume no outflow of electronic current; thus,

$$\mathbf{i}_{\mathrm{s}} \cdot \mathbf{n} = 0. \tag{2.46}$$

Also, assuming that for all ionic species the convective flux in the axial direction of the felt is dominant, the sum of the migrative and diffusive fluxes is set to zero, i.e.

$$-D_k^{\mathrm{eff}}\left(\frac{z_k c_k F}{RT}\nabla\phi_{\mathrm{e}} + \nabla c_k\right)\cdot\mathbf{n} = 0, \quad k = \mathrm{H}^+, \mathrm{HSO}_4^-, \mathrm{SO}_4^{2-}, \mathrm{V}^{2+}, \mathrm{V}^{3+}. \tag{2.47}$$

Combining (2.47) with the electroneutrality condition (2.4) gives

$$-D_k^{\mathrm{eff}}\nabla c_k \cdot \mathbf{n} = 0, \quad k = \mathrm{H}^+, \mathrm{HSO}_4^-, \mathrm{SO}_4^{2-}, \mathrm{V}^{2+}, \mathrm{V}^{3+}, \tag{2.48}$$

$$\nabla\phi_{\mathrm{e}} \cdot \mathbf{n} = 0. \tag{2.49}$$

*2.2.8 Positive electrode inlet (**9**)*

Here, at $y = 0$, $h_m/2 \leq x \leq h_f + h_m/2$,

$$\mathbf{i}_s \cdot \mathbf{n} = 0, \tag{2.50}$$

$$c_k = c_k^{in}(t), \quad k = H^+, HSO_4^-, SO_4^{2-}, VO_2^+, VO^{2+}, \tag{2.51}$$

where c_k^{in} is the positive electrode inlet ionic concentration for species k, and is given by (2.43), where $c_k^{out}(t)$ is given by (2.44), but with the upper and lower limits replaced by $h_m/2 + h_f$ and $h_m/2$, respectively.

*2.2.9 Positive electrode outlet (**10**)*

Here, at $y = L, h_m/2 \leq x \leq h_f + h_m/2$,

$$\mathbf{i}_s \cdot \mathbf{n} = 0, \tag{2.52}$$

$$-D_k^{eff} \nabla c_k \cdot \mathbf{n} = 0, \quad k = H^+, HSO_4^-, SO_4^{2-}, VO_2^+, VO^{2+}, \tag{2.53}$$

$$\nabla \phi_e \cdot \mathbf{n} = 0. \tag{2.54}$$

2.3 Initial conditions

At $t = 0$: for the negative electrode, i.e. region **I**,

$$c_k = c_k^0 \text{ for } k = H^+, HSO_4^-, SO_4^{2-}, V^{2+}, V^{3+}; \tag{2.55}$$

for the positive electrode, i.e. region **III**,

$$c_k = c_k^0 \text{ for } i = H^+, HSO_4^-, SO_4^{2-}, VO_2^+, VO^{2+}. \tag{2.56}$$

It is convenient to associate the vanadium-related quantities to the initial concentrations of the electrolytes in the positive electrode and negative electrode tanks, $c^0_{VOSO_4}$ and $c^0_{V_2(SO_4)_3}$ respectively, and the initially prescribed state of charge, SOC^0. In particular, for the negative electrode,

$$c^0_{V^{2+}} = SOC^0 c^0_{V_2(SO_4)_3}, \quad c^0_{V^{3+}} = \left(1 - SOC^0\right) c^0_{V_2(SO_4)_3}, \tag{2.57}$$

whereas at the positive electrode,

$$c^0_{VO_2^+} = SOC^0 c^0_{VOSO_4}, \quad c^0_{VO^{2+}} = \left(1 - SOC^0\right) c^0_{VOSO_4}. \tag{2.58}$$

Furthermore, whilst c_k^0 can be determined for $k = V^{2+}, V^{3+}, VO_2^+, VO^{2+}$ by considering the concentrations of the electrolytes, it is also necessary to prescribe c_k^0 for $k = H^+, HSO_4^-, SO_4^{2-}$; for these, $c^0_{SO_4^{2-}}$ should be specified, whereas $c^0_{H^+}$ and $c^0_{HSO_4^-}$ must satisfy $r_d = 0$.

2.4 Summary

At this stage, the model equations are as follows:

- (2.3),(2.4),(2.9),(2.10) and (2.23) as the governing equations for

$$c_{\mathrm{H}^+}, c_{\mathrm{HSO}_4^-}, c_{\mathrm{SO}_4^{2-}}, c_{\mathrm{V}^{2+}}, c_{\mathrm{V}^{3+}}, c_{\mathrm{VO}_2^+}, c_{\mathrm{VO}^{2+}}, \phi_{\mathrm{e}}, \phi_{\mathrm{m}}, \phi_{\mathrm{s}};$$

- (2.25)-(2.34),(2.36),(2.38),(2.40)-(2.43) and (2.46)-(2.54) as the boundary conditions;
- (2.55)-(2.58) as the initial conditions.

3 Nondimensionalization

To nondimensionalize, we set

$$X = \frac{x}{h_{\mathrm{f}}}, \quad Y = \frac{y}{L}, \quad \tau = \frac{t}{V/\omega\Lambda}, \quad \Phi_{\mathrm{e}} = \frac{\phi_{\mathrm{e}}}{[\phi]}, \quad \Phi_{\mathrm{s}} = \frac{\phi_{\mathrm{s}}}{[\phi]},$$
$$\mathbf{I}_{\mathrm{s}} = \frac{\mathbf{i}_{\mathrm{s}}}{\left[i_{\mathrm{app}}\right]}, \quad \mathbf{I}_{\mathrm{e}} = \frac{\mathbf{i}_{\mathrm{e}}}{\left[i_{\mathrm{app}}\right]}, \quad I_{\mathrm{app}} = \frac{i_{\mathrm{app}}}{\left[i_{\mathrm{app}}\right]}, \quad J_{\pm} = \frac{j_{\pm}}{\left[i_{\mathrm{app}}\right]/h_{\mathrm{f}}}, \tag{3.1}$$

where

$$\Lambda = \frac{L\left[i_{\mathrm{app}}\right]}{c_{\mathrm{H}^+}^{0,-} u^{\mathrm{in}} h_{\mathrm{f}} F}, \quad [\phi] = \frac{\left[i_{\mathrm{app}}\right] h_{\mathrm{f}}}{\sigma_{\mathrm{s}}^{\mathrm{eff}}},$$

and, for $k = \mathrm{H}^+, \mathrm{HSO}_4^-, \mathrm{SO}_4^{2-}, \mathrm{V}^{2+}, \mathrm{V}^{3+}, \mathrm{VO}^{2+}, \mathrm{VO}_2^+$,

$$C_k = \frac{c_k}{c_{\mathrm{H}^+}^{0,-}}, \quad \hat{S}_k = \frac{S_k}{\left[i_{\mathrm{app}}\right]/h_{\mathrm{f}}F}, \quad \hat{R}_k = \frac{R_k}{c_{\mathrm{H}^+}^{0,-} u^{\mathrm{in}}/L}, \tag{3.2}$$

where $c_{\mathrm{H}^+}^{0,-}$ is the initial H^+ concentration at the negative electrode and $\left[i_{\mathrm{app}}\right] = \max_t(i_{\mathrm{app}}(t))$. Since typically $h_{\mathrm{f}}/L \ll 1$, Eq. (2.3) becomes

$$\varepsilon\chi\frac{\partial C_k}{\partial\tau} + \frac{\partial C_k}{\partial Y} = \frac{\mathscr{D}_k}{Pe}\frac{\partial}{\partial X}\left(z_k\Pi C_k\frac{\partial\Phi_{\mathrm{e}}}{\partial X} + \frac{\partial C_k}{\partial X}\right) - \Lambda\hat{S}_k - \Theta\hat{R}_k, \tag{3.3}$$

where

$$Pe = \frac{h_{\mathrm{f}}^2 u^{\mathrm{in}}}{L D_{\mathrm{H}^+}^{\mathrm{eff}}}, \quad \Pi = \frac{F[\phi]}{RT}, \quad \mathscr{D}_k = \frac{D_k^{\mathrm{eff}}}{D_{\mathrm{H}^+}^{\mathrm{eff}}}, \quad \chi = \frac{L^2\omega\left[i_{\mathrm{app}}\right]}{(u^{\mathrm{in}})^2 V c_{\mathrm{H}^+}^{0,-} h_{\mathrm{f}} F}, \quad \Theta = \frac{Lk_d}{c_{\mathrm{H}^+}^{0,-} u^{\mathrm{in}}}, \tag{3.4}$$

whereas (2.43) becomes

$$\frac{\mathrm{d}C_k^{\mathrm{in}}}{\mathrm{d}\tau} = \frac{1}{\Lambda}\left(C_k^{\mathrm{out}}(\tau) - C_k^{\mathrm{in}}(\tau)\right). \tag{3.5}$$

Of all of the governing equations, boundary conditions and initial conditions, we have only focused here on (3.3) and (3.5), as they are the only ones that contain dimensionless parameters whose values are key for the forthcoming analysis. Instead, we note that, on using the data in Tables 3-6, we have

$$Pe \sim 230, \quad \Pi \sim 0.9, \quad \Lambda \sim 1.5\times10^{-3}, \quad \chi \sim 1.1\times10^{-4}, \quad \Theta \sim 166. \tag{3.6}$$

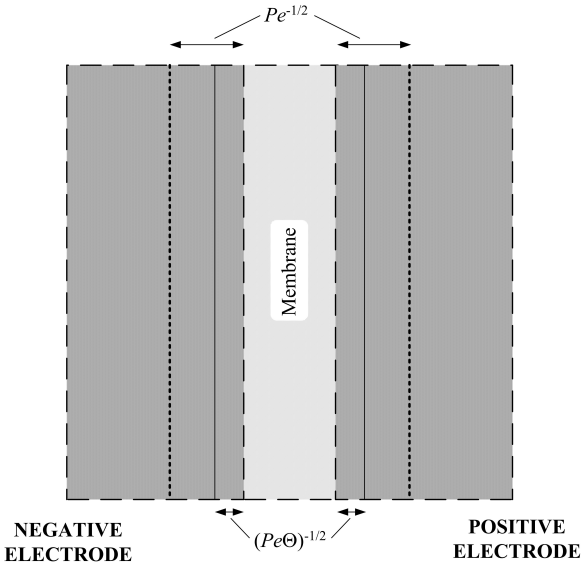

Fig. 3 A schematic for the overall asymptotic structure for the model with H_2SO_4 dissociation

4 Analysis

4.1 Overview

At this point, we indicate in general terms how the analysis will proceed. As in [16], the whole problem can be decomposed hierarchically, giving the following sequence:

1. $C^{\text{in}}_{\text{H}^+}, C^{\text{in}}_{\text{HSO}_4^-}, C^{\text{in}}_{\text{SO}_4^{2-}}, C^{\text{in}}_{\text{V}^{2+}}, C^{\text{in}}_{\text{V}^{3+}}$ for the negative electrode, and hence for the bulk;
2. $C^{\text{in}}_{\text{H}^+}, C^{\text{in}}_{\text{HSO}_4^-}, C^{\text{in}}_{\text{SO}_4^{2-}}, C^{\text{in}}_{\text{VO}^{2+}}, C^{\text{in}}_{\text{VO}_2^+}$ for the positive electrode, and hence for the bulk;
3. $\Phi_{\text{e}}, \Phi_{\text{s}}$ in the negative electrode;
4. $\Phi_{\text{e}}, \Phi_{\text{s}}$ in the positive electrode;
5. $C_{\text{H}^+}, C_{\text{HSO}_4^-}, C_{\text{SO}_4^{2-}}, C_{\text{V}^{2+}}, C_{\text{V}^{3+}}$ in a reaction layer of width $(Pe\Theta)^{-1/2}$ near $X = -\mathscr{H}$ in the negative electrode;
6. $C_{\text{H}^+}, C_{\text{HSO}_4^-}, C_{\text{SO}_4^{2-}}, C_{\text{V}^{2+}}, C_{\text{V}^{3+}}$ in a boundary layer of width $Pe^{-1/2}$ near $X = -\mathscr{H}$ in the negative electrode;
7. $C_{\text{H}^+}, C_{\text{HSO}_4^-}, C_{\text{SO}_4^{2-}}, C_{\text{VO}^{2+}}, C_{\text{VO}_2^+}$ in a reaction layer of width $(Pe\Theta)^{-1/2}$ near $X = \mathscr{H}$ in the positive electrode;
8. $C_{\text{H}^+}, C_{\text{HSO}_4^-}, C_{\text{SO}_4^{2-}}, C_{\text{VO}^{2+}}, C_{\text{VO}_2^+}$ in a boundary layer of width $Pe^{-1/2}$ near $X = \mathscr{H}$ in the positive electrode.

However, the introduction of the dissociation reaction complicates the items that were present in [16] - 1,2,3,4,6 and 8 - as well as introducing two new items - 5 and 7. To understand how these steps are linked, it is instructive to consider the schematic shown in Fig. 3, which depicts the bulk regions and the boundary layers. Moreover, in

order to determine the cell potential, E_{cell}, during charging and discharging, it proves to be only necessary to calculate steps 1-4, as was the case in [16]; for this reason, in what follows, we will not perform any computations related to steps 5-8, although we will indicate how they are related asymptotically to steps 1-4.

Item 1 is dealt with in Sects. 4.2 and 4.3, item 2 in Sect. 4.5 and items 3 and 4 in Sect. 4.4.

4.2 Negative electrode (I)

Here, as governing equations, we have (3.3) for $k = \text{H}^+, \text{HSO}_4^-, \text{SO}_4^{2-}, \text{V}^{2+}, \text{V}^{3+}$,

$$\varepsilon\chi\frac{\partial C_k}{\partial \tau} + \frac{\partial C_k}{\partial Y} = \frac{\mathscr{D}_k}{Pe}\frac{\partial}{\partial X}\left(z_k \Pi C_k \frac{\partial \Phi_{\text{e}}}{\partial X} + \frac{\partial C_k}{\partial X}\right) - \Lambda \hat{S}_k - \Theta \hat{R}_k, \tag{4.1}$$

and the electroneutrality condition,

$$\sum_{\substack{k=\text{H}^+,\text{HSO}_4^-,\text{SO}_4^{2-},\\ \text{V}^{2+},\text{V}^{3+}}} z_k C_k = 0. \tag{4.2}$$

Also, we note from (2.9) and (2.10) that

$$\frac{\partial}{\partial X}\left(I_{s,X} + I_{e,X}\right) + \delta\frac{\partial}{\partial Y}\left(I_{s,Y} + I_{e,Y}\right) = 0, \tag{4.3}$$

where $\delta = h_{\text{f}}/L$ and $I_{\text{e},X}/\,I_{\text{s},X}$ and $I_{\text{e},Y}/\,I_{\text{s},Y}$ are the X- and Y-components, respectively, of $\mathbf{I}_{\text{e}}/\mathbf{I}_{\text{s}}$. Now, because $\delta \ll 1$, (4.3) reduces to

$$\frac{\partial}{\partial X}\left(I_{\text{e},X} + I_{\text{s},X}\right) \approx 0, \tag{4.4}$$

as discussed previously in [16]. Next, using (2.38) and (4.4), we have

$$I_{\text{e},X} + I_{\text{s},X} \equiv I_{\text{app}}(\tau) \quad \text{for } -(1+\mathscr{H}) \leq X \leq -\mathscr{H}, \tag{4.5}$$

where $\mathscr{H} = h_{\text{m}}/2h_{\text{f}}$. Also, since (2.27) implies that $I_{\text{s},X} = 0$ at $X = -\mathscr{H}$, we must also have $I_{\text{e},X} = I_{\text{app}}(\tau)$. Hence, the boundary conditions at $X = -\mathscr{H}$ are

$$\mathscr{D}_k\left(z_k C_k \Pi\frac{\partial \Phi_{\text{e}}}{\partial X} + \frac{\partial C_k}{\partial X}\right) = \begin{cases} 0, & k = \text{HSO}_4^-, \text{SO}_4^{2-}, \text{V}^{2+}, \text{V}^{3+} \\ \Omega I_{\text{app}}(\tau), & k = \text{H}^+, \end{cases}, \tag{4.6}$$

where $\Omega = \left[i_{\text{app}}\right] h_{\text{f}}/z_{\text{H}^+} c_{\text{H}^+}^{0,-} D_{\text{H}^+}^{\text{eff}} F$ and, at $X = -(1+\mathscr{H})$,

$$z_k C_k \Pi\frac{\partial \Phi_{\text{e}}}{\partial X} + \frac{\partial C_k}{\partial X} = 0 \quad \text{for } k = \text{H}^+, \text{HSO}_4^-, \text{SO}_4^{2-}, \text{V}^{2+}, \text{V}^{3+}. \tag{4.7}$$

From (3.6), we have that $Pe \gg 1, \Theta \gg 1, \Lambda \ll 1, \chi \ll 1$, so that (4.1) reduces, at leading order, to

$$\frac{\partial C_k}{\partial Y} \approx 0, \quad k = \text{V}^{2+}, \text{V}^{3+}, \tag{4.8}$$

$$\hat{R}_k \approx 0, \quad k = \text{H}^+, \text{HSO}_4^-, \text{SO}_4^{2-}; \tag{4.9}$$

thence, $C_k \equiv C_k(X,\tau)$ for $k = \mathrm{V}^{2+}, \mathrm{V}^{3+}$, and hence

$$C_k \equiv C_k^{\mathrm{in}}(\tau), \quad k = \mathrm{V}^{2+}, \mathrm{V}^{3+}, \tag{4.10}$$

in view of the nondimensional version of (2.42), whereas (4.9) implies that

$$C_{\mathrm{H}^+} \approx \frac{C_{\mathrm{HSO}_4^-}}{\mathscr{B}}, \tag{4.11}$$

where $\mathscr{B} = (1-\beta)/(1+\beta)$. From electroneutrality, we now have

$$\left(z_{\mathrm{H}^+} + \mathscr{B} z_{\mathrm{HSO}_4^-}\right) C_{\mathrm{H}^+} + C_{\mathrm{SO}_4^{2-}} = -z_{\mathrm{V}^{2+}} C_{\mathrm{V}^{2+}}(\tau) - z_{\mathrm{V}^{3+}} C_{\mathrm{V}^{3+}}(\tau), \tag{4.12}$$

which indicates that the linear combination of C_{H^+} and $C_{\mathrm{SO}_4^{2-}}$ on the left-hand side should be a function of τ. Whilst this still leaves the possibility that C_{H^+} and $C_{\mathrm{SO}_4^{2-}}$ can both be functions of X, Y and τ, the simpler alternative, which is borne out by the later computations, is that they are just functions of τ, and thence

$$C_k \equiv C_k^{\mathrm{in}}(\tau), \quad k = \mathrm{H}^+, \mathrm{HSO}_4^-, \mathrm{SO}_4^{2-}, \tag{4.13}$$

as for $k = \mathrm{V}^{2+}, \mathrm{V}^{3+}$. Now, multiplying (4.1) by z_k, summing, using electroneutrality, Eq. (4.10) and

$$\sum_{\substack{k=\mathrm{H}^+,\mathrm{HSO}_4^-,\mathrm{SO}_4^{2-},\\ \mathrm{V}^{2+},\mathrm{V}^{3+}}} z_k \hat{R}_k = 0, \tag{4.14}$$

we obtain

$$\Gamma_-(\tau) \frac{\partial^2 \Phi_{\mathrm{e}}}{\partial X^2} = -J_-, \tag{4.15}$$

where we use the fact that $\hat{S}_k = s_k J_-$, and with

$$\Gamma_-(\tau) = \lambda \sum_{\substack{k=\mathrm{H}^+,\mathrm{HSO}_4^-,\mathrm{SO}_4^{2-},\\ \mathrm{V}^{2+},\mathrm{V}^{3+}}} z_k^2 \mathscr{D}_k C_k^{\mathrm{in}}(\tau), \tag{4.16}$$

where $\lambda := \Pi/\Lambda Pe \sim O(1)$. Note also at this point that we have, from the dimensionless form of the second equation in (2.9), Ohm's law, i.e. Eq. (2.7), and the nondimensional electronic current density in Eq. (3.2),

$$\frac{\partial^2 \Phi_{\mathrm{s}}}{\partial X^2} = J_-. \tag{4.17}$$

Recall also that J_- is a function of Φ_{e} and Φ_{s}, so that (4.15) and (4.17) will be coupled.

As regards boundary conditions for (4.15) and (4.17), we have, for Φ_{s},

$$\frac{\partial \Phi_{\mathrm{s}}}{\partial X} = 0 \quad \text{at } X = -\mathscr{H}, \tag{4.18}$$

$$\frac{\partial \Phi_{\mathrm{s}}}{\partial X} = I_{\mathrm{app}}(\tau) \quad \text{at } X = -(1+\mathscr{H}). \tag{4.19}$$

As for $\Phi_{\rm e}$, we can use (4.7) and electroneutrality to obtain

$$\frac{\partial \Phi_{\rm e}}{\partial X} = 0 \quad \text{at } X = -(1+\mathscr{H}). \tag{4.20}$$

However, we still need a boundary condition for $\Phi_{\rm e}$ at $X = -\mathscr{H}$; this is not entirely straightforward to derive, since we cannot simply replace C_k by $C_k^{\rm in}(\tau)$ in Eqs. (4.6) and (4.7) without justification, in view of the nested boundary-layer structure that was indicated in Fig. 3. Presently, in Sect. 4.4, the required condition will be shown to be Eq. (4.53), which in fact has the same form as that in [16], even though the boundary-layer structure there was not of nested type.

Since the right-hand side of (4.15) depends on $\Phi_{\rm e}, \Phi_{\rm s}, C^{\rm in}_{\rm V^{2+}}$ and $C^{\rm in}_{\rm V^{3+}}$, and since the latter two are functions of τ only, it is clear that there is a self-consistent solution structure for which $\Phi_{\rm e}$ and $\Phi_{\rm s}$ are functions only of X and τ, and not of Y.

4.3 $C_{\rm H^+}, C_{\rm HSO_4^-}, C_{\rm V^{2+}}, C_{\rm V^{3+}}, C_{\rm SO_4^{2-}}$ in the bulk

Integrating (4.1) over $-(1+\mathscr{H}) \leq X \leq -\mathscr{H}$ and applying boundary conditions (4.6) and (4.7), we obtain

$$\left(\varepsilon\chi\frac{\partial}{\partial\tau}+\frac{\partial}{\partial Y}\right)\left(\int_{-(1+\mathscr{H})}^{-\mathscr{H}} C_k \,{\rm d}X\right) = -\Lambda s_k \int_{-(1+\mathscr{H})}^{-\mathscr{H}} J_- \,{\rm d}X, \quad \text{for } k = {\rm V^{2+}}, {\rm V^{3+}}. \tag{4.21}$$

Integrating (4.21) over $0 \leq Y \leq 1$ and using the result from the supplementary material in [16] that

$$\int_{-(1+\mathscr{H})}^{-\mathscr{H}} J_- \,{\rm d}X = -z_{\rm H^+} I_{\rm app}(\tau), \tag{4.22}$$

we see that

$$\varepsilon\chi\frac{\partial}{\partial\tau}\left(\int_0^1\int_{-(1+\mathscr{H})}^{-\mathscr{H}} C_k \,{\rm d}X\,{\rm d}Y\right) + C_k^{\rm out} - C_k^{\rm in} = \Lambda z_{\rm H^+} s_k I_{\rm app}(\tau), \quad \text{for } k = {\rm V^{2+}}, {\rm V^{3+}}, \tag{4.23}$$

where we have used

$$\int_{-(1+\mathscr{H})}^{-\mathscr{H}} C_k|_{Y=0}^{Y=1} \,{\rm d}X = C_k^{\rm out} - C_k^{\rm in}. \tag{4.24}$$

Also, from (3.5), we have

$$\varepsilon\Delta\frac{\rm d}{{\rm d}\tau}\left(\int_0^1\int_{-(1+\mathscr{H})}^{-\mathscr{H}} C_k \,{\rm d}X\,{\rm d}Y\right) + \frac{{\rm d}C_k^{\rm in}}{{\rm d}\tau} = z_{\rm H^+} s_k, \tag{4.25}$$

where $\Delta = \chi/\Lambda \ (\ll 1)$. Note that although C_k for all k, as proposed in (4.10), and $\Phi_{\rm e}$, as proposed in (4.15), would satisfy all of the boundary conditions at $X = -(1+\mathscr{H})$, they would not be able to satisfy all of the boundary conditions at $X = -\mathscr{H}$. Thus, a boundary-layer structure is necessary near $X = -\mathscr{H}$; we give the details of this in Sect. 4.4.

Equation (4.25) identifies Δ as a small parameter, and it is appropriate at this juncture to introduce a regular perturbation expansion for $\varphi = (C_k, C_k^{\text{in}})$ in the form

$$\varphi = \varphi_0 + \Delta\varphi_1 + O\left(\Delta^2\right). \tag{4.26}$$

Thus, we obtain, from (4.25) and the dimensionless form of (2.55) at $O(1)$,

$$C_{k,0}^{\text{in}} = C_k^0 + z_{\text{H}^+} s_k \int_0^\tau I_{\text{app}}\left(\tau'\right) \mathrm{d}\tau', \quad \text{for } k = \text{V}^{2+}, \text{V}^{3+}. \tag{4.27}$$

For later use, we will also need $C_{k,1}^{\text{in}}$, which satisfies, on considering Eq. (4.25) at $O(\Delta)$,

$$\frac{\mathrm{d}C_{k,1}^{\text{in}}}{\mathrm{d}\tau} = -\varepsilon \frac{\mathrm{d}C_{k,0}^{\text{in}}}{\mathrm{d}\tau}, \tag{4.28}$$

subject to

$$C_{k,1}^{\text{in}} = 0 \quad \text{at } \tau = 0, \tag{4.29}$$

which comes from the dimensionless form of (2.55) at $O(\Delta)$; thence, $C_{k,1}^{\text{in}}$ is easily found to be

$$C_{k,1}^{\text{in}} = -s_k \varepsilon \int_0^\tau I_{\text{app}}\left(\tau'\right) \mathrm{d}\tau'. \tag{4.30}$$

Note that the expressions in (4.27) and (4.30) have turned out to be identical to the corresponding ones in [16], meaning that SOC_- in Eq. (2.45) will also be identical.

Similarly, integrating (4.1) for $k = \text{H}^+, \text{HSO}_4^-, \text{SO}_4^{2-}$, we obtain

$$\left(\varepsilon\chi\frac{\partial}{\partial\tau} + \frac{\partial}{\partial Y}\right)\left(\int_{-(1+\mathscr{H})}^{-\mathscr{H}} C_k \mathrm{d}X\right) = -\Theta \int_{-(1+\mathscr{H})}^{-\mathscr{H}} \hat{R}_k \mathrm{d}X; \tag{4.31}$$

integrating over $0 \le Y \le 1$, we obtain

$$\varepsilon\chi\frac{\partial}{\partial\tau}\left(\int_0^1 \int_{-(1+\mathscr{H})}^{-\mathscr{H}} C_k \mathrm{d}X\mathrm{d}Y\right) + C_k^{\text{out}} - C_k^{\text{in}} = -\Theta \int_0^1 \int_{-(1+\mathscr{H})}^{-\mathscr{H}} \hat{R}_k \mathrm{d}X\mathrm{d}Y. \tag{4.32}$$

From (3.5), we have

$$\varepsilon\Delta\frac{\partial}{\partial\tau}\left(\int_0^1 \int_{-(1+\mathscr{H})}^{-\mathscr{H}} C_k \mathrm{d}X\mathrm{d}Y\right) + \frac{\mathrm{d}C_k^{\text{in}}}{\mathrm{d}\tau} = -\frac{\Theta}{\Lambda}\int_0^1 \int_{-(1+\mathscr{H})}^{-\mathscr{H}} \hat{R}_k \mathrm{d}X\mathrm{d}Y. \tag{4.33}$$

We can now note that

$$\sum_{k=\text{HSO}_4^-, \text{SO}_4^{2-}} \left\{\varepsilon\Delta\frac{\partial}{\partial\tau}\left(\int_0^1 \int_{-(1+\mathscr{H})}^{-\mathscr{H}} C_k \mathrm{d}X\mathrm{d}Y\right) + \frac{\mathrm{d}C_k^{\text{in}}}{\mathrm{d}\tau}\right\} = 0, \tag{4.34}$$

whereupon we obtain

$$C_{\text{HSO}_4^-,0}^{\text{in}}(\tau) + C_{\text{SO}_4^{2-},0}^{\text{in}}(\tau) = C_{\text{HSO}_4^-}^0 + C_{\text{SO}_4^{2-}}^0 \tag{4.35}$$

and

$$C_{\text{HSO}_4^-,1}^{\text{in}}(\tau) + C_{\text{SO}_4^{2-},1}^{\text{in}}(\tau) = 0. \tag{4.36}$$

With (4.11) implying that

$$C^{\text{in}}_{\text{H}^+,0}(\tau) = \frac{C^{\text{in}}_{\text{HSO}_4^-,0}(\tau)}{\mathscr{B}}, \quad C^{\text{in}}_{\text{H}^+,1}(\tau) = \frac{C^{\text{in}}_{\text{HSO}_4^-,1}(\tau)}{\mathscr{B}}, \tag{4.37}$$

we find from electroneutrality that

$$C^{\text{in}}_{\text{H}^+,0}(\tau) = 1 - \frac{z_{\text{H}^+}\mathscr{I}_-(\tau)}{z_{\text{H}^+} + \mathscr{B}\left(z_{\text{HSO}_4^-} - z_{\text{SO}_4^{2-}}\right)}, \tag{4.38}$$

$$C^{\text{in}}_{\text{H}^+,1}(\tau) = \frac{\varepsilon\mathscr{I}_-(\tau)}{z_{\text{H}^+} + \mathscr{B}\left(z_{\text{HSO}_4^-} - z_{\text{SO}_4^{2-}}\right)}, \tag{4.39}$$

where

$$\mathscr{I}_-(\tau) = \left(z_{\text{V}^{2+}}s_{\text{V}^{2+}} + z_{\text{V}^{3+}}s_{\text{V}^{3+}}\right)\int_0^\tau I_{\text{app}}\left(\tau'\right)\mathrm{d}\tau',$$

and thence

$$C^{\text{in}}_{\text{HSO}_4^-,0}(\tau) = \mathscr{B}\left(1 - \frac{z_{\text{H}^+}\mathscr{I}_-(\tau)}{z_{\text{H}^+} + \mathscr{B}\left(z_{\text{HSO}_4^-} - z_{\text{SO}_4^{2-}}\right)}\right), \tag{4.40}$$

$$C^{\text{in}}_{\text{HSO}_4^-,1}(\tau) = \frac{\mathscr{B}\varepsilon\mathscr{I}_-(\tau)}{z_{\text{H}^+} + \mathscr{B}\left(z_{\text{HSO}_4^-} - z_{\text{SO}_4^{2-}}\right)}, \tag{4.41}$$

$$C^{\text{in}}_{\text{SO}_4^{2-},0}(\tau) = C^0_{\text{HSO}_4^-} + C^0_{\text{SO}_4^{2-}} - \mathscr{B}\left(1 - \frac{z_{\text{H}^+}\mathscr{I}_-(\tau)}{z_{\text{H}^+} + \mathscr{B}\left(z_{\text{HSO}_4^-} - z_{\text{SO}_4^{2-}}\right)}\right), \tag{4.42}$$

$$C^{\text{in}}_{\text{SO}_4^{2-},1}(\tau) = -\frac{\mathscr{B}\varepsilon\mathscr{I}_-(\tau)}{z_{\text{H}^+} + \mathscr{B}\left(z_{\text{HSO}_4^-} - z_{\text{SO}_4^{2-}}\right)}. \tag{4.43}$$

Observe also that the corresponding equations in [16] for (4.38)-(4.43) were

$$C^{\text{in}}_{\text{H}^+,0}(\tau) = 1 - z_{\text{H}^+}\mathscr{I}_-(\tau), \tag{4.44}$$

$$C^{\text{in}}_{\text{H}^+,1}(\tau) = \varepsilon z_{\text{H}^+}\mathscr{I}_-(\tau), \tag{4.45}$$

$$C^{\text{in}}_{\text{HSO}_4^-,0}(\tau) = C^0_{\text{HSO}_4^-}, \tag{4.46}$$

$$C^{\text{in}}_{\text{HSO}_4^-,1}(\tau) = 0, \tag{4.47}$$

$$C^{\text{in}}_{\text{SO}_4^{2-},0}(\tau) = C^0_{\text{SO}_4^{2-}}, \tag{4.48}$$

$$C^{\text{in}}_{\text{SO}_4^{2-},1}(\tau) = 0. \tag{4.49}$$

Thus, there is no single substitution that can be used in (4.38)-(4.43) so as to obtain (4.44)-(4.49); the closest rule that can be arrived at is to set $\mathscr{B}$ to zero if it is in a term that contains $\mathscr{I}_-(\tau)$, but to use (4.11) and set $\mathscr{B} = C^0_{\text{HSO}_4^-}$ otherwise.

4.4 Ionic potential, $\Phi_{\rm e}$, and electronic potential, $\Phi_{\rm s}$

Having determined $C_k^{\rm in}(\tau)$ to $O(\Delta)$, we return to the problem of determining $\Phi_{\rm e}$, recalling that this satisfies (4.15), subject to (4.20) and a condition at $X=-\mathscr{H}$ which we have yet to establish. To determine this, we need to consider the boundary-layer structure near $X=-\mathscr{H}$; this has already been signposted in Fig. 3, although we give the analytical justification here.

As in [16], we set

$$X=-\left(\mathscr{H}+Pe^{-1/2}\hat{X}\right),\quad \Phi_{\rm e}=\Phi_{\rm e}(Y,-\mathscr{H},\tau)+\Pi^{-1}\bar{\Phi}_{\rm e}\left(\hat{X},Y,\tau\right),$$
$$C_k=\hat{C}_k,\quad k=\mathrm{H}^+,\mathrm{HSO}_4^-,\mathrm{SO}_4^{2-},\mathrm{V}^{2+},\mathrm{V}^{3+}, \tag{4.50}$$

where Π was defined in Eq. (3.4), Eqs. (4.1) gives, at leading order, for $0<\hat{X}<\infty$,

$$\frac{\partial\hat{C}_k}{\partial Y}=\mathscr{D}_k\frac{\partial}{\partial\hat{X}}\left(z_k\hat{C}_k\frac{\partial\bar{\Phi}_{\rm e}}{\partial\hat{X}}+\frac{\partial\hat{C}_k}{\partial\hat{X}}\right)-\Lambda\hat{S}_k-\Theta\hat{R}_k,\quad k=\mathrm{H}^+,\mathrm{HSO}_4^-,\mathrm{SO}_4^{2-},\mathrm{V}^{2+},\mathrm{V}^{3+}; \tag{4.51}$$

observe that $\Phi_{\rm e}(Y,-\mathscr{H},\tau)$ is not yet known at this stage, but there is no need to know it yet either, since it does not appear in (4.51). Recalling that $\Lambda\ll1$ and $\Theta\gg1$ suggests that we can neglect the next to last term on the right-hand side of (4.51), but must retain the last one. However, multiplying (4.51) by z_k, summing and applying electroneutrality, we obtain

$$\sum_{\substack{k=\mathrm{H}^+,\mathrm{HSO}_4^-,\mathrm{SO}_4^{2-},\\ \mathrm{V}^{2+},\mathrm{V}^{3+}}} z_k\mathscr{D}_k\frac{\partial}{\partial\hat{X}}\left(z_k\hat{C}_k\frac{\partial\bar{\Phi}_{\rm e}}{\partial\hat{X}}+\frac{\partial\hat{C}_k}{\partial\hat{X}}\right)=0, \tag{4.52}$$

since $\Lambda\ll1$ and in view of (4.14); then, integrating (4.52) with respect to $\hat{X}$ indicates that

$$\sum_{\substack{k=\mathrm{H}^+,\mathrm{HSO}_4^-,\mathrm{SO}_4^{2-},\\ \mathrm{V}^{2+},\mathrm{V}^{3+}}} z_k\mathscr{D}_k\left(z_k\hat{C}_k\frac{\partial\bar{\Phi}_{\rm e}}{\partial\hat{X}}+\frac{\partial\hat{C}_k}{\partial\hat{X}}\right)$$

is a function of Y and τ. We observe that the above expression is the X-component of the nondimensional ionic current density, $\mathbf{I}_{\rm e}$, which was defined in (3.2); this result indicates that $\mathbf{I}_{\rm e}$ is conserved across the boundary layer. This is sufficient for us to be able to use the boundary condition at $X=-\mathscr{H}$, which is clearly well inside the boundary layer, as a boundary condition for the ionic current density in the bulk of the electrolyte; as a consequence,

$$\Gamma_-(\tau)\frac{\partial\Phi_{\rm e}}{\partial X}=I_{\rm app}(\tau)\quad\text{at } X=-\mathscr{H}. \tag{4.53}$$

However, notice that prior to summing (4.51) over k, we have

$$\hat{R}_k\approx0\quad\text{for } k=\mathrm{H}^+,\mathrm{HSO}_4^-,\mathrm{SO}_4^{2-},$$

at leading order, since $\Theta \gg 1$. This would simply lead to $\hat{C}_{\mathrm{H}^+} = \hat{C}_{\mathrm{HSO}_4^-}/\mathscr{B}$, and it is impossible that a solution based around this identity could satisfy all of the boundary conditions given in (4.6). Consequently, there has to be a nested boundary layer for which $\hat{X} \sim \Theta^{-1/2}$, in which the diffusion term in (4.51) balances the chemical reaction term; thus, overall, we have that $X \sim (Pe\Theta)^{-1/2}$ in this layer, as shown in Fig. 3. We do not document the resulting equations for this layer, as there is no need to solve them, as far as the leading-order problem is concerned; physically, the ionic species that participate in the chemical reaction, i.e. $\mathrm{H}^+, \mathrm{HSO}_4^-, \mathrm{SO}_4^{2-}$, vary rapidly across this layer, but with advection playing a negligible role. With hindsight, the mathematical similarities between the VRFB model with and without acid dissociation follow very closely those in multi-ion models for the electrolytic pickling of steel with and without bulk chemical reactions [29–32], even though the two situations are very different. First of all, it should be recalled that in the earlier models for electrolytic pickling, it is only the ionic current that is solved for, whereas here, for a porous electrode, we solve for both ionic and electronic currents; thus, there is an additional field equation, i.e. for the electronic potential, which is not present in the pickling models. Second, in electrolytic pickling, the ionic current at leading order is a constant across the entire domain between two electrodes, whereas here, it is only constant across the concentration boundary layer. Third, the electrolytic pickling models were for a steady state, whereas the current VRFB model is time-dependent.

To re-cap, solving (4.15), (4.17)-(4.20) and (4.53) will determine Φ_{e} and Φ_{s} in the negative electrode, and in particular Φ_{e} at $X = -\mathscr{H}$. We can then find Φ_{m}^-, i.e. Φ_{m} at $X = -\mathscr{H}$, from the nondimensional version of (2.30), that is

$$\Phi_{\mathrm{m}}^- = \Phi_{\mathrm{e}} - \frac{1}{\Pi}\left[-\ln C_{\mathrm{H}^+}\right]_-^+. \tag{4.54}$$

Next, denoting the value of C_{H^+} inside the membrane, $c_{\mathrm{fcs}}/c_{\mathrm{H}^+}^{0,-}$, as $C_{\mathrm{H}^+,\mathrm{m}}$, we see from (2.23) that

$$-\frac{z_{\mathrm{H}^+}^2 F^2 c_{\mathrm{H}^+}^{0,-}}{RTh_{\mathrm{m}}}[\phi]\, D_{\mathrm{H}^+,\mathrm{m}} C_{\mathrm{H}^+,\mathrm{m}}\left(\Phi_{\mathrm{m}}^+ - \Phi_{\mathrm{m}}^-\right) = I_{\mathrm{app}}(\tau), \tag{4.55}$$

which gives Φ_{m} at $X = \mathscr{H}$; denoting this by Φ_{m}^+, we have

$$\Phi_{\mathrm{m}}^+ = \Phi_{\mathrm{e}} - \frac{1}{\Pi}\left[\ln C_{\mathrm{H}^+}\right]_-^+, \tag{4.56}$$

i.e. this will give Φ_{e} at $X = \mathscr{H}$ also. Note that, by this stage, we have determined the potentials for the negative electrode and the membrane without having to determine those in the positive electrode; however, we need to find them there in order to determine the cell potential, and we thus turn to the positive electrode.

4.5 Positive electrode (III)

Here, as governing equations, we have (3.3) for $k = \mathrm{H}^+, \mathrm{HSO}_4^-, \mathrm{SO}_4^{2-}, \mathrm{VO}^{2+}, \mathrm{VO}_2^+$,

$$\varepsilon\chi\frac{\partial C_k}{\partial \tau} + \frac{\partial C_k}{\partial Y} = \frac{\mathscr{D}_k}{Pe}\frac{\partial}{\partial X}\left(z_k \Pi C_k \frac{\partial \Phi_{\mathrm{e}}}{\partial X} + \frac{\partial C_k}{\partial X}\right) - \Lambda \hat{S}_k - \Theta \hat{R}_k, \tag{4.57}$$

and the electroneutrality condition,

$$\sum_{\substack{k=\mathrm{H}^+,\mathrm{HSO}_4^-,\mathrm{SO}_4^{2-},\\ \mathrm{VO}^{2+},\mathrm{VO}_2^+}} z_k C_k = 0. \tag{4.58}$$

The boundary conditions at $X = \mathscr{H}$ are

$$\mathscr{D}_k \left(z_k \Pi C_k \frac{\partial \Phi_\mathrm{e}}{\partial X} + \frac{\partial C_k}{\partial X} \right) = \begin{cases} 0, & k = \mathrm{HSO}_4^-, \mathrm{SO}_4^{2-}, \mathrm{VO}^{2+}, \mathrm{VO}_2^+ \\ \Omega I_\mathrm{app}(\tau), & k = \mathrm{H}^+, \end{cases}, \tag{4.59}$$

and, at $X = 1 + \mathscr{H}$,

$$z_k \Pi C_k \frac{\partial \Phi_\mathrm{e}}{\partial X} + \frac{\partial C_k}{\partial X} = 0 \quad \text{for } k = \mathrm{H}^+, \mathrm{HSO}_4^-, \mathrm{SO}_4^{2-}, \mathrm{VO}^{2+}, \mathrm{VO}_2^+. \tag{4.60}$$

For this electrode also, the solution can be determined hierarchically. We skip the majority of the details, which are similar to those for the negative electrode. For Φ_e and Φ_s, we have

$$\Gamma_+(\tau) \frac{\partial^2 \Phi_\mathrm{e}}{\partial X^2} = -J_+, \tag{4.61}$$

$$\frac{\partial^2 \Phi_\mathrm{s}}{\partial X^2} = J_+, \tag{4.62}$$

respectively, where we have used the fact that $\hat{S}_k = s_k J_+$, and where

$$\Gamma_+(\tau) = \lambda \sum_{\substack{k=\mathrm{H}^+,\mathrm{HSO}_4^-,\mathrm{SO}_4^{2-},\\ \mathrm{VO}^{2+},\mathrm{VO}_2^+}} z_k^2 \mathscr{D}_k C_k^\mathrm{in}(\tau); \tag{4.63}$$

Eqs. (4.61) and (4.62) are subject to the boundary conditions

$$-\Gamma_+(\tau) \frac{\partial \Phi_\mathrm{e}}{\partial X} = I_\mathrm{app}(\tau), \quad \frac{\partial \Phi_\mathrm{s}}{\partial X} = 0 \quad \text{at } X = \mathscr{H}, \tag{4.64}$$

$$\frac{\partial \Phi_\mathrm{e}}{\partial X} = 0, \quad \frac{\partial \Phi_\mathrm{s}}{\partial X} = I_\mathrm{app}(\tau) \quad \text{at } X = 1 + \mathscr{H}. \tag{4.65}$$

Also, we have, for $k = \mathrm{VO}^{2+}, \mathrm{VO}_2^+$,

$$\varepsilon \Delta \frac{\partial}{\partial \tau} \left(\int_0^1 \int_\mathscr{H}^{1+\mathscr{H}} C_k \mathrm{d}X \mathrm{d}Y \right) + \frac{\mathrm{d}C_k^\mathrm{in}}{\mathrm{d}\tau} = -s_k \int_\mathscr{H}^{1+\mathscr{H}} J_+ \mathrm{d}X, \tag{4.66}$$

and, for $k = \mathrm{HSO}_4^-, \mathrm{SO}_4^{2-}$,

$$\varepsilon \Delta \frac{\partial}{\partial \tau} \left(\int_0^1 \int_\mathscr{H}^{1+\mathscr{H}} C_k \mathrm{d}X \mathrm{d}Y \right) + \frac{\mathrm{d}C_k^\mathrm{in}}{\mathrm{d}\tau} = -\frac{\Theta}{\Lambda} \int_0^1 \int_{-(1+\mathscr{H})}^{-\mathscr{H}} \hat{R}_k \mathrm{d}X \mathrm{d}Y, \tag{4.67}$$

whence

$$C^{\text{in}}_{\text{H}^+,0}(\tau) = C^{0,+}_{\text{H}^+} - \frac{z_{\text{H}^+}\mathscr{I}_+(\tau)}{z_{\text{H}^+} + \mathscr{B}\left(z_{\text{HSO}_4^-} - z_{\text{SO}_4^{2-}}\right)}, \tag{4.68}$$

$$C^{\text{in}}_{\text{HSO}_4^-,0}(\tau) = \mathscr{B}\left(C^{0,+}_{\text{H}^+} - \frac{z_{\text{H}^+}\mathscr{I}_+(\tau)}{z_{\text{H}^+} + \mathscr{B}\left(z_{\text{HSO}_4^-} - z_{\text{SO}_4^{2-}}\right)}\right), \tag{4.69}$$

$$C^{\text{in}}_{\text{SO}_4^{2-},0}(\tau) = C^{0}_{\text{HSO}_4^-} + C^{0}_{\text{SO}_4^{2-}} - \mathscr{B}\left(C^{0,+}_{\text{H}^+} - \frac{z_{\text{H}^+}\mathscr{I}_+(\tau)}{z_{\text{H}^+} + \mathscr{B}\left(z_{\text{HSO}_4^-} - z_{\text{SO}_4^{2-}}\right)}\right), \tag{4.70}$$

$$C^{\text{in}}_{\text{VO}^{2+},0}(\tau) = C^{0}_{\text{VO}^{2+}} + z_{\text{H}^+}s_{\text{VO}^{2+}}\int_0^\tau I_{\text{app}}(\tau')\,\mathrm{d}\tau', \tag{4.71}$$

$$C^{\text{in}}_{\text{VO}_2^+,0}(\tau) = C^{0}_{\text{VO}_2^+} + z_{\text{H}^+}s_{\text{VO}_2^+}\int_0^\tau I_{\text{app}}(\tau')\,\mathrm{d}\tau', \tag{4.72}$$

where $C^{0,+}_{\text{H}^+} = c^{0,+}_{\text{H}^+}/c^{0,-}_{\text{H}^+}$, with $c^{0,+}_{\text{H}^+}$ as the initial H^+ concentration at the positive electrode, and

$$C^{\text{in}}_{\text{H}^+,1}(\tau) = \frac{\varepsilon\mathscr{I}_+(\tau)}{z_{\text{H}^+} + \mathscr{B}\left(z_{\text{HSO}_4^-} - z_{\text{SO}_4^{2-}}\right)}, \tag{4.73}$$

$$C^{\text{in}}_{\text{HSO}_4^-,1}(\tau) = \frac{\mathscr{B}\varepsilon\mathscr{I}_+(\tau)}{z_{\text{H}^+} + \mathscr{B}\left(z_{\text{HSO}_4^-} - z_{\text{SO}_4^{2-}}\right)}, \tag{4.74}$$

$$C^{\text{in}}_{\text{SO}_4^{2-},1}(\tau) = -\frac{\mathscr{B}\varepsilon\mathscr{I}_+(\tau)}{z_{\text{H}^+} + \mathscr{B}\left(z_{\text{HSO}_4^-} - z_{\text{SO}_4^{2-}}\right)}, \tag{4.75}$$

$$C^{\text{in}}_{\text{VO}^{2+},1}(\tau) = -z_{\text{H}^+}s_{\text{VO}^{2+}}\varepsilon\int_0^\tau I_{\text{app}}(\tau')\,\mathrm{d}\tau', \tag{4.76}$$

$$C^{\text{in}}_{\text{VO}_2^+,1}(\tau) = -z_{\text{H}^+}s_{\text{VO}_2^+}\varepsilon\int_0^\tau I_{\text{app}}(\tau')\,\mathrm{d}\tau', \tag{4.77}$$

with

$$\mathscr{I}_+(\tau) = \left(s_{\text{VO}_2^+}z_{\text{VO}_2^+} + s_{\text{VO}^{2+}}z_{\text{VO}^{2+}}\right)\int_0^\tau I_{\text{app}}(\tau')\,\mathrm{d}\tau'.$$

Again, note that the expressions in (4.71),(4.72),(4.76) and (4.77) have turned out to be the same as the corresponding ones in [16], meaning that SOC_+ in Eq. (2.45) will also be identical; this was perhaps not to have been expected, since H^+ participates both in the electrochemical reaction and in acid dissociation reaction. Observe also

that the corresponding equations in [16] for (4.68)-(4.70) and (4.73)-(4.75) were

$$C^{\mathrm{in}}_{\mathrm{H}^+,0}(\tau) = C^{0,+}_{\mathrm{H}^+} - z_{\mathrm{H}^+}\mathscr{I}_+(\tau), \tag{4.78}$$

$$C^{\mathrm{in}}_{\mathrm{HSO}_4^-,0}(\tau) = C^{0}_{\mathrm{HSO}_4^-}, \tag{4.79}$$

$$C^{\mathrm{in}}_{\mathrm{SO}_4^{2-},0}(\tau) = C^{0}_{\mathrm{SO}_4^{2-}}, \tag{4.80}$$

$$C^{\mathrm{in}}_{\mathrm{H}^+,1}(\tau) = \frac{\varepsilon z_{\mathrm{H}^+}\mathscr{I}_+(\tau)}{z_{\mathrm{H}^+} + \mathscr{B}\left(z_{\mathrm{HSO}_4^-} - z_{\mathrm{SO}_4^{2-}}\right)}, \tag{4.81}$$

$$C^{\mathrm{in}}_{\mathrm{HSO}_4^-,1}(\tau) = 0, \tag{4.82}$$

$$C^{\mathrm{in}}_{\mathrm{SO}_4^{2-},1}(\tau) = 0, \tag{4.83}$$

respectively. As for the negative electrode, there is no single substitution that can be used in (4.38)-(4.43) so as to obtain (4.44)-(4.49). This time, setting $\mathscr{B}$ to zero if it is in a term that contains $\mathscr{I}_+(\tau)$,but using (4.11) and setting $\mathscr{B} = C^0_{\mathrm{HSO}_4^-}/C^{0+}_{\mathrm{H}^{+}-}$ otherwise, will reduce (4.68)-(4.70) and (4.73)-(4.75) to (4.78)-(4.83), respectively.

5 Results

Two numerical tasks remain:

A) the solution of the transient 2D model, consisting of Eqs. (2.3),(2.4),(2.9),(2.10), and (2.23), subject to Eqs. (2.25)-(2.34),(2.36),(2.38),(2.40)-(2.43) and (2.46)-(2.58);
B) the solution of the asymptotic problem derived in Sects. 4.2-4.5, which consists of Eqs. (4.15),(4.17),(4.61), and (4.62), subject to Eqs. (4.18)-(4.20),(4.53),(4.64) and (4.65), with input for $\Gamma_\pm(\tau)$ and $J_\pm(\tau)$ coming from Eqs. (4.27),(4.30),(4.38)-(4.43) and (4.68)-(4.77).

These are tackled are in the same way as given in the supplementary material of [16], and the details are therefore not presented here; however, we mention in passing that the 250-fold saving in computational time when using the asymptotically reduced model, as compared to the original formulated transient 2D model, was again noted. Instead, we move on towards a presentation of the results. In what follows, we consider solutions for the galvanostatic case, so that i_{app} is constant during charging and discharging, giving

$$\int_0^\tau I_{\mathrm{app}}(\tau')\,\mathrm{d}\tau' = \tau. \tag{5.1}$$

Also, to enable a fair comparison between the results of the models with and without dissociation, we have taken the same criterion for setting the charge time in the current model as was used in the 2D transient model in [16], as this enables us to use those results directly. In turn, the criterion used in [16] was that the state of charge, SOC, should reach 0.95. Thanks to the asymptotic analysis in [16], it was found that the two expressions for SOC given in Eq. (2.45) collapsed onto each for the results presented there; indeed, from Eqs. (4.27),(4.30),(4.71),(4.72),(4.76) and (4.77),

it is clear that this will also be the case here. Moreover, although nondimensional variables have served their purpose in helping to identify leading-order asymptotic simplifications, we return to dimensional variables, for the most part, for considering actual model results.

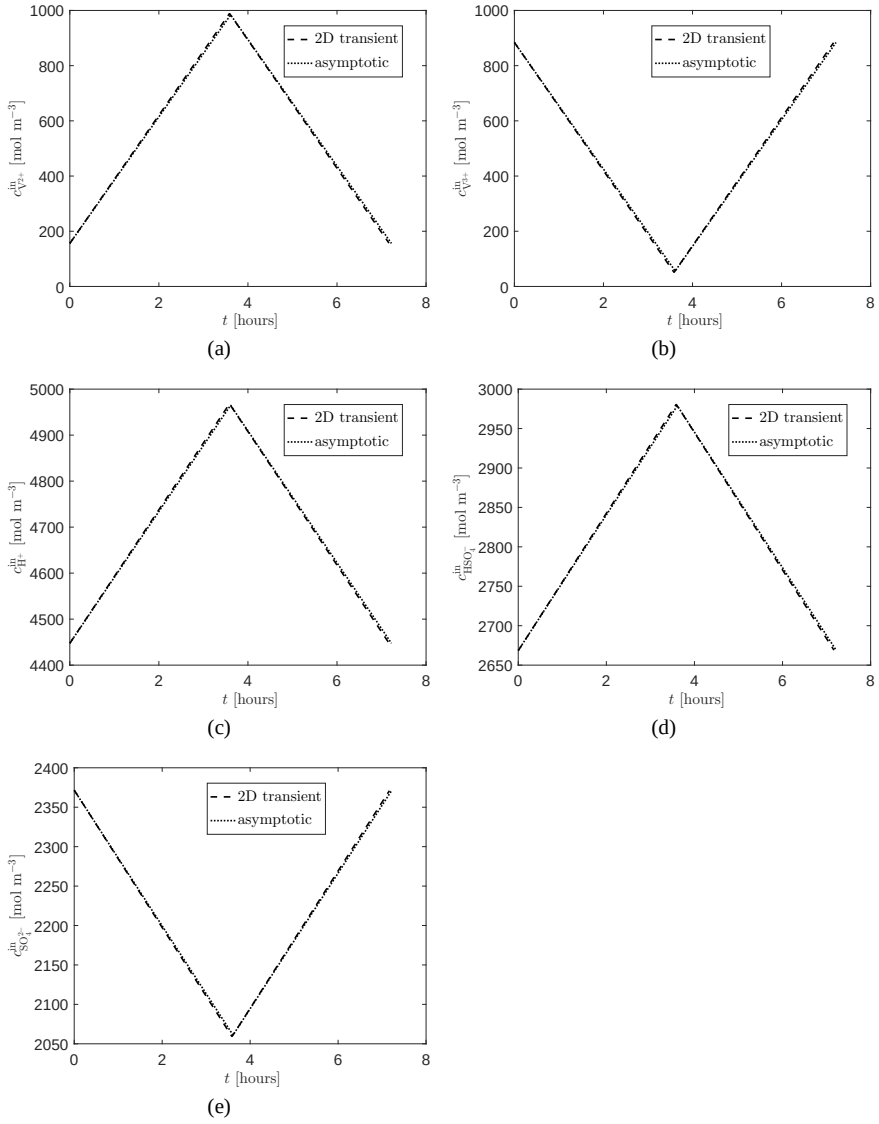

Fig. 4 Inlet concentrations at the negative electrode as functions of time, t : (a) $c^{\text{in}}_{V^{2+}}$; (b) $c^{\text{in}}_{V^{3+}}$; (c) $c^{\text{in}}_{H^{+}}$; (d) $c^{\text{in}}_{HSO_4^-}$; (e) $c^{\text{in}}_{SO_4^{2-}}$

5.1 Model with acid dissociation

Fig. 4(a)-(e) show the inlet concentration for the various species at the negative electrode as functions of time, t, for the 2D transient and two-term asymptotic models. For all species, it is evident that both models predict a linear evolution, and that the agreement between the two models is very good. We point out that we do not plot the solutions from the one-term asymptotic model, as this was already found to be not accurate enough for the model without acid dissociation in [16]. Essentially, this is because $\Delta\,(\sim 0.1)$, although being treated as asymptotically small, is not numerically small enough; in fact, the results were found to be so inaccurate in [16] as to predict near total depletion of V^{3+} and VO_2^+ ions during charging. Similarly, Fig. 5(a)-(e) shows a comparison of the the inlet concentration for the various species at the positive electrode. Moreover, if we focus on the (a) and (b) plots in Figs. 4 and 5 and use the equations in (2.45) for the state of charge, we observe that $\mathrm{SOC}_+ = \mathrm{SOC}_-$, as was also the case in [16].

Fig. 6 shows the charge-discharge curve at a current density of 400 A m^{-2} for 2D transient and two-term asymptotic model predictions; as in [16], the agreement is very good, even though we have appended an additional bulk reaction to the model.

5.2 Comparison with the no-dissociation model

It is of interest to compare the results of the models with and without dissociation. We do not do this for all inlet profiles this time, but just select $c^{\mathrm{in}}_{H^+}$ for both electrodes. The comparison of the two-term asymptotic profiles is shown in Fig. 7. Thus, we see that during charging/discharging, $c^{\mathrm{in}}_{H^+}$ for the negative electrode increases/decreases more slowly if dissociation is taken into account, whilst $c^{\mathrm{in}}_{H^+}$ for the positive electrode increases/decreases more quickly if dissociation is taken into account. As regards the other ions:

- the $c^{\mathrm{in}}_{V^{2+}}$,$c^{\mathrm{in}}_{V^{3+}}$, $c^{\mathrm{in}}_{VO^{2+}}$ and $c^{\mathrm{in}}_{VO_2^+}$ profiles are unaffected;
- whereas $c^{\mathrm{in}}_{HSO_4^-}$ and $c^{\mathrm{in}}_{SO_4^{2-}}$ remain constant when dissociation is neglected, they increase/decrease linearly during charging, and decrease/increase linearly during discharging.

In addition, in Fig. 8, we compare the charge-discharge curve from the asymptotic model in [16] with the curve from the asymptotic model in Fig. 6; here also, we find the two curves to be more or less identical, meaning that the inclusion of the dissociation reaction appears to have no net effect on these curves.

To understand why the charge-discharge curves in Fig. 8 appear to be so similar, it suffices to consider $J_\pm$ and $\Gamma_\pm$ in the two asymptotic models; thus, for this, we return to nondimensional variables. First of all, referring back to Eqs. (2.11), (2.13), (2.14) and (2.16), we can note that J_- is identical in the two models, since $c^{\mathrm{in}}_{V^{2+}}$ and $c^{\mathrm{in}}_{V^{3+}}$ are, as seen in Fig. 4(a) and (b). On the other hand, referring back to Eqs. (2.12), (2.13), (2.15) and (2.17), we can expect that there should be a difference in J_+, because $c^{\mathrm{in}}_{H^+}$ in the positive electrodes is different in the two models, as seen in Fig. 5(a). Similarly,

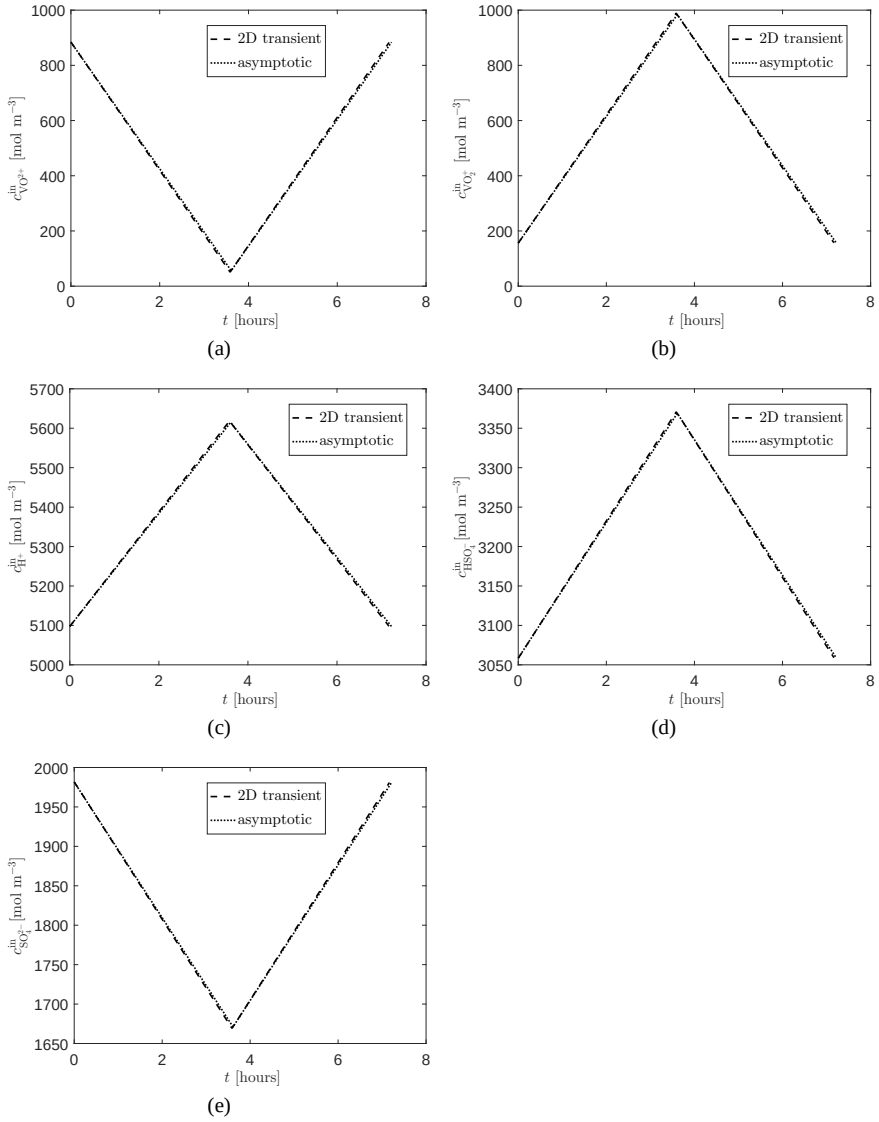

Fig. 5 Inlet concentrations at the positive electrode as functions of time, t : (a) $c^{\text{in}}_{\text{VO}^{2+}}$; (b) $c^{\text{in}}_{\text{VO}_2^+}$; (c) $c^{\text{in}}_{\text{H}^+}$; (d) $c^{\text{in}}_{\text{HSO}_4^-}$; (e) $c^{\text{in}}_{\text{SO}_4^{2-}}$

we would expect $\Gamma_{\pm}$ to be different, since they both contain $c^{\text{in}}_{\text{H}^+}$, $c^{\text{in}}_{\text{HSO}_4^-}$ and $c^{\text{in}}_{\text{SO}_4^{2-}}$, whose profiles change significantly when dissociation is included. $\Gamma_{\pm}$ are plotted as functions of τ in Fig. 9, and it is clear that, although each profile is slightly affected by the dissociation reaction, the effect is insignificant as regards generating a substantial enough difference in the charge-discharge curve is concerned.

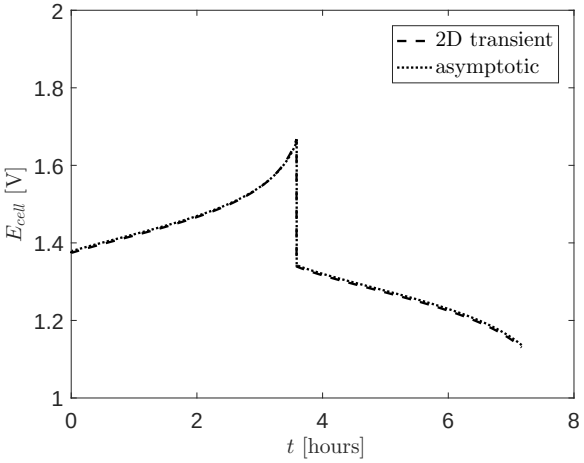

Fig. 6 Charge-discharge curve at a current density of 400 A m^{-2} , as predicted by the 2D transient and the asymptotic models

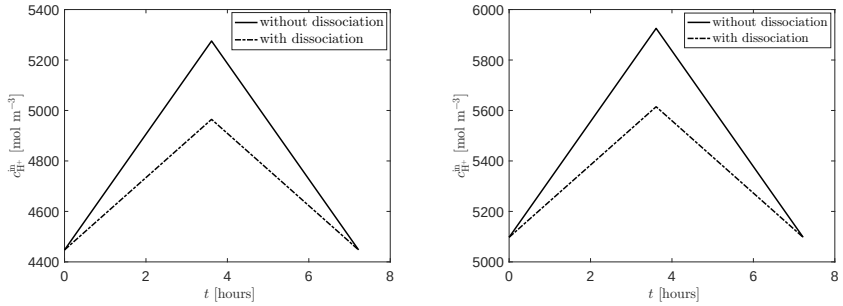

Fig. 7 Comparison of $c^{\text{in}}_{\text{H}^+}$ for the asymptotic models with and without acid dissociation: (a) negative electrode; (b) positive electrode

Lastly, we consider a comparison of the model results with available experimental data, which would normally be done via charge-discharge curve data. As seen in Fig. 8, the results we have obtained for the cell potential as a function of time are more or less identical to those in [16], where a comparison with experimental data obtained when $i_{\text{app}} = 400$ Am^{-2} was made; see Fig. 4 therein. As the agreement was reasonable but not perfect, it was suggested that a way to improve it would be to adjust the value of E_{cell} upwards by 0.04V, as had been done previously in [18], where the required adjustment, of 0.072 V, had been even greater; the rationale for this was that because open circuit voltages are not able to behave in a standard Butler-Volmer-type way, this may have a large impact on E_{cell}. These comments notwithstanding, the model in [9] gave much better agreement than either the model in [16] or that in [18]; it was suggested in [16] that this may have been due to the fact that extra

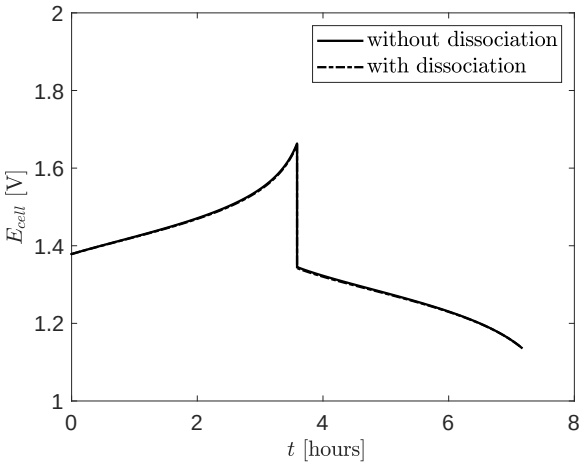

Fig. 8 Charge-discharge curve at a current density of 400 A m^{-2}, including and excluding the dissociation of sulphuric acid, as predicted by the asymptotic model

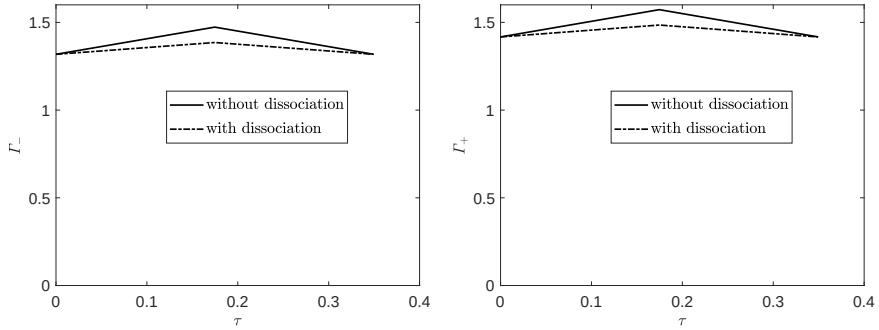

(a) (b)

Fig. 9 (a) Γ_- as a function of dimensionless time, τ; (b) Γ_+ as a function of dimensionless time, τ

physics, in the form of acid dissociation and vanadium crossover, had been included, although it would have been difficult to tell whether these factors are decisive since no attempt was made in [9] to compare against a model that did not include these effects. In consequence, the current work at least rules out acid dissociation as a factor in the discrepancy. Here, however, we expand the discussion regarding experimental validation a little further, by considering comparison against a different data set and at two differing applied current densities [3]; the details are given in appendix A.

6 Conclusions

This paper has used asymptotic and numerical methods to extend a recent 2D transient model for the operation of a vanadium redox flow battery [16], so as to include

the dissociation of sulphuric acid in the battery's porous flow-through electrodes. As in the earlier model, it was found that asymptotic analysis was able to recover the solution structure that is present in the full model. In addition, the analysis was able to explain why the charge-discharge curve remains unaffected by whether acid dissociation is included or not, even though the concentrations of the ionic species in the recirculating tanks, although not the state of charge, are considerably different in the two models.

Moreover, the fact that it has been possible to add extra physics onto the base model, whilst still making use of the original asymptotic framework, provides hope that further phenomena that are believed to be of importance in VRFB modelling - oxygen and hydrogen evolution, thermal effects, vanadium crossover - can be accommodated in the same way.

Acknowledgement

The second author acknowledges the financial support of FAPESP (Fundação de Amparo à Pesquisa do Estado de São Paulo) for the researcher grant [Grant Number 2016/12678-0].

Appendix A: Model validation against experimental data from [3]

For the purposes of validating our model, we use experimental data from You et al. [3], who provide the cell potential as a function of state of charge for charging and discharging at 400 and 800 Am^{-2}; the comparison is shown in Fig. A.1. The agreement is very good for the charging phase, although less so for the discharging phase, where it is in line with the comparison against this experimental data made by Chen et al. [11], albeit it only at 400 Am^{-2}. It can be noted that You et al. [3] also presented a model which gave the best agreement of all at both 400 and 800 Am^{-2}, although a shift in cell potential of 140 mV was required to achieve it; here, we have not employed any shift. Note also that we have used the same model data as in [3], although with the value for active surface area - A in equations (2.11) and (2.12) - given in [9].

Lastly, we point out that, even though the model is now being used for a completely different set of parameter values, and in particular for a much higher applied current density, the agreement between the results of the 2D transient model and the reduced asymptotic model remains very good.

References

1. Shah AA, Watt-Smith MJ, Walsh FC (2008) A dynamic performance model for redox-flow batteries involving soluble species. Electrochimica Acta 53:8087–8100
2. Al-Fetlawi A, Shah AA, Walsh FC (2009) Non-isothermal modelling of the all-vanadium redox-flow battery. Electrochimica Acta 55:78–89
3. You D, Zhang H, Chen J (2009) A simple model for the vanadium redox battery. Electrochimica Acta 54:6827–6836

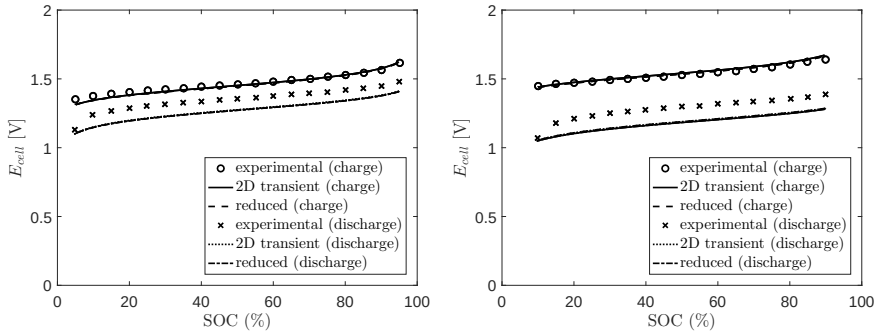

Fig. A.1 Cell potential, E_{cell}, as a function of state of charge, SOC, during charge and discharge from experiments [3], the 2D transient model and the 2-term reduced asymptotic model at a current density, i_{app}, of: (a) 400 Am^{-2}; (b) 800 Am^{-2}

4. Al-Fetlawi A, Shah AA, Walsh FC (2010) Modelling the effects of oxygen evolution in the all-vanadium redox flow battery. Electrochimica Acta 55:3192–3205
5. Shah AA, Al-Fetlawi H, Walsh FC (2010) Dynamic modelling of hydrogen evolution effects in the all-vanadium redox flow battery. Electrochimica Acta 55:1125–1139
6. Shah AA, Tangirala R, Singh R, Wills RGA, Walsh FC (2011) A Dynamic unit cell model for the all-vanadium flow battery. J Electrochem Soc 158 (6):A671–A677
7. Knehr K, Kumbur EC (2011) Open circuit voltage of vanadium redox flow batteries: Discrepancy between models and experiments. Electrochem Commun 13:342–345
8. Ma X, Zhang H, Xing F (2011) A three-dimensional model for negative half cell of the vanadium redox flow battery. Electrochimica Acta 58:238–246
9. Knehr KW, Agar E, Dennison CR, Kalidindi AR, Kumbur EC (2012) A Transient Vanadium Flow Battery Model Incorporating Vanadium Crossover and Water Transport through the Membrane. J Electrochem Soc 159 (9):A1446–A1459
10. Tang A, Bao J, Skyllas-Kazacos M (2012) Thermal modelling of battery configuration and self-discharge reactions in vanadium redox flow battery. J Power Sources 216:489–501
11. Chen CL, Yeoh HK, Chakrabarti MH (2014) An enhancement to Vynnycky's model for the all-vanadium redox flow battery. Electrochimica Acta 120:167–179
12. Zheng Q, Zhang H, Xing F, Ma X, Li X, Ning G (2014) A three-dimensional model for thermal analysis in a vanadium flow battery. Applied Energy 113:1675 – 1685
13. Oh K, Yoo H, Ko J, Won S, Ju H (2015) Three-dimensional, transient, nonisothermal model of all-vanadium redox flow batteries. Energy 81:3–14
14. Xu Q, Zhao TS, Zhang C (2014) Effects of SOC-dependent electrolyte viscosity on performance of vanadium redox flow batteries. Applied Energy 130:139–147
15. Xu Q, Zhao TS (2015) Fundamental models for flow batteries. Prog Energy Comb Sci 49:40–58
16. Vynnycky M, Assunção M (2019) The vanadium redox flow battery: an asymptotic perspective. SIAM J Appl Math 79:1147–1172
17. Gattrell M, Park J, MacDougall B, Apte J, McCarthy S, Wu CM (2004) Study of the mechanism of the vanadium $4+/5+$ redox reaction in acidic solutions. J Electrochem Soc 151:A123–A130
18. Sharma AK, Vynnycky M, Ling CY, Birgersson E, Han M (2014) The quasi-steady state of all-vanadium redox flow batteries: A scale analysis. Electrochimica Acta 147:657–662
19. Sharma AK, Ling CY, Birgersson E, Vynnycky M, Han M (2015) Verified reduction of dimensionality for an all-vanadium redox flow battery model. J Power Sources 279:345–350
20. Comsol Multiphysics 5.4, http://www.comsol.com
21. Vynnycky M (2011) Analysis of a model for the operation of a vanadium redox battery. Energy 36:2242–2256
22. Assunção M (2015) Mathematical modelling of vanadium redox batteries. Master's thesis, KTH Royal Institute of Technology, Stockholm, Sweden
23. Bernardi DM, Verbrugge MW (1991) Mathematical model of a gas diffusion electrode bonded to a polymer electrolyte. AIChe J 37:1151–1163

24. Pourbaix M (1974) Atlas of electrochemical equilibria in aqueous solutions. 2nd edition. NACE, Houston, TX
25. Knopf DA, Luo BP, Krieger UK, Koop T (2003) Thermodynamic dissociation constant of the bisulfate ion from Raman and ion interaction modeling studies of aqueous sulfuric acid at low temperatures. J Phys Chem A 107 (21):4322–4332
26. Newman JS, Thomas-Alyea KE (2004) Electrochemical Systems. 3rd edition. John Wiley & Sons, New Jersey
27. Lide DR (2003) Handbook of Chemistry and Physics. 84th edition. CRC Press, Inc. Boca Raton, Florida
28. Yamamura T, Watanabe N, Yano T, Shiokawa Y (2005) Electron transfer kinetics of Np^{3+}/Np^{4+}, NpO_2^+/NpO_2^{2+}, V^{2+}/V^{3+}, and VO^{2+}/VO_2^+ at carbon electrodes. J Electrochem Soc 152:A830–A836
29. Vynnycky M, Ipek N (2009) Supporting electrolyte asymptotics and the electrochemical pickling of steel. Proc Roy Soc A 465:3771–3797
30. Vynnycky M (2011) Correction to: Supporting electrolyte asymptotics and the electrochemical pickling of steel (Proc. R. Soc. A, 465 (2009) 3771-3797). Proc R Soc A 467:3035–3037
31. Vynnycky M, Ipek N (2011) Reaction-layer asymptotics and the electrochemical pickling of steel. Proc R Soc A 467:2534–2560
32. Vynnycky M, Ipek N (2013) Multiple bulk-reaction asymptotics and the electrochemical pickling of steel. J Engng Maths 80:105–128